CURRENT TREND IN SYNTHESIS, POST-SYNTHETIC MODIFICATIONS AND BIOLOGICAL APPLICATIONS OF NANOMETAL-ORGANIC FRAMEWORKS (NMOFs)

Ebenezer Baa[a*], Gary M. Watkins[b], Rui. W. Krause[c] and Derek. N. Tantoh[d]

[a,b,c]Rhodes University, Department of Chemistry, South Africa

[a] ebenezerbaa@yahoo.com

[b] g.watkins@ru.ac.za

[c] r.krause@ru.ac.za

[*] corresponding author

[d]University of Johannesburg, Department of Applied Chemistry; South Africa

dndinteh@uj.ac.za

Abstract

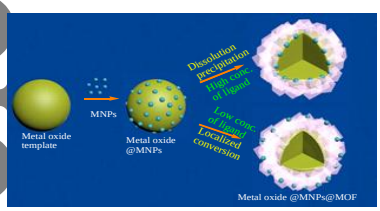

Since the early reports of MOFs and their interesting properties, research involving these materials has grown wide in scope and applications. Various synthetic approaches have ensued in view of obtaining materials with optimised properties, the extensive scope of application spanning from energy, gas sorption, catalysis biological applications has meant exponentially evolved over the years. The far-reaching synthetic and PSM approaches and porosity control possibilities have continued to serve as a motivation for research on these materials. With respect to the biological applications, MOFs have shown promise as good candidates in applications involving drug delivery, BioMOFs, sensing, imaging amongst others. Despite being a while away from successful entry into the market, observed results in sensing, drug delivery, and imaging put these materials on the spot light as candidates poised to usher in a revolution in biology. In this regard, this review article focuses current approaches in synthesis, post functionalization and biological applications of these materials with particular attention on drug delivery, imaging, sensing and BioMOFs.

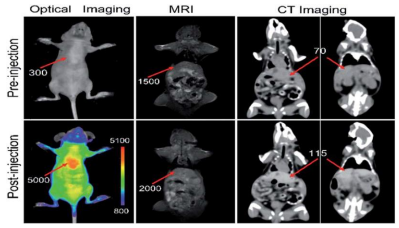

Key words: MOFs, postsynthetic modification, imaging, BioMOFs, sensing.

Table of Contents

1. Introduction

Metal–organic frameworks (MOFs), also known as porous coordination net-works (PCNs) or porous coordination polymers (PCPs), have emerged as a new class of porous crystalline generally obtained by linking metal ions or clusters (usually known as Secondary building units, SBUs) and organic linkers [1–3] . Although the porosity of these materials cannot always be guaranteed [4], when they however do, these materials are known to have well defined pores and large internal surface area, properties which make them suitable candidates for interesting application. MOFs possess amorphous [5–7] or crystalline structures with well-defined supramolecular architectures [8], wherein the metal ions or clusters are linked to the linkers by means of coordinate bonds to give rise to material with either 1D, 2D or 3D network [9–11]. This novel class of materials has received considerable attention in the industry and research in the last decades due to their many potential applications in several important areas including gas storage, separation, catalysis, photonics, environmental conservation, heterogeneous catalysis, luminescent materials, biomedicine, ion exchange and more recently as light weight molecular sieves amongst others. These potential applications mostly stem from the inherent large internal surface areas, tuneable pore sizes and topologies which lead to versatile architectures [11].

MOFs typically are bioinorganic in nature with the organic aspect

This article has been accepted for publication and undergone full peer review but has not been through the copyediting, typesetting, pagination and proofreading process, which may lead to differences between this version and the Version of Record. Please cite this article as doi: 10.1002/cjoc.201800407

arising from the ligand and inorganic from metal ions or clusters used. This dual nature further renders them more attractive for various applications where organic and inorganic components act in synergy. The extensive range of possible organic linkers and variety of metal ions or clusters that can be used to assemble these MOFs [12] and additionally the possibility of modifications [3], leads to an almost endless range of MOFs structures that can be obtained [13]. This versatility has led to several journal articles published in the last two decades on the subject (Figure 2) following the pioneering works of Yaghi et al [14,15], Kitagawa et al [16] and Ferey et al [17] amongst others. MOF materials unlike traditional inorganic materials can be synthesized from well-defined molecular building blocks, due to both the relative ease of molecular synthesis and advantage of crystal engineering by means of hierarchical organization [14,15]. There exist a vast repertoire of published literature of synthetic and characterization approaches to MOFs with most of the research however more experimental in nature and directed to synthesis of new structures. In light of the development and revolutionary potential, molecular modelling studies have also been employed to explore both synthetic approaches and application in such areas as gas storage and separation which are two areas considered to be quite attractive for the application of MOFs [19].

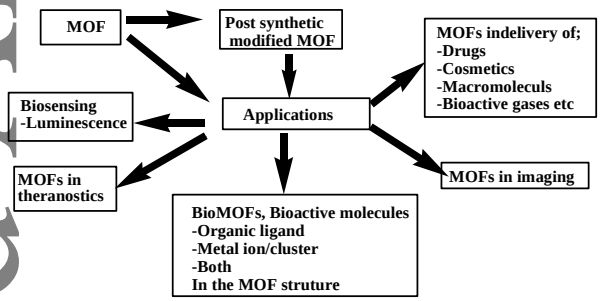

Figure 1: Biological applications of MOFs

The physical and chemical versatility arising from judicious choice of linkers and metal ions/clusters of MOFs make MOF materials good candidates for several bio-application that range from "delivery vehicles" to theranostics and imaging amongst other applications [19]. In light of this advantage, research has veered on the synthesis and application in biological systems. It is worth noting however that despite this unprecedented potential in bio-application, MOFs are still a while away from being in the market in this domain. In this review, we examine the current state of synthetic approaches for bio-applications, bio-applications avenues, factors affecting bio-applications and the future perspectives of MOFs in bio-applications with particular interest on nanoscale MOFs.

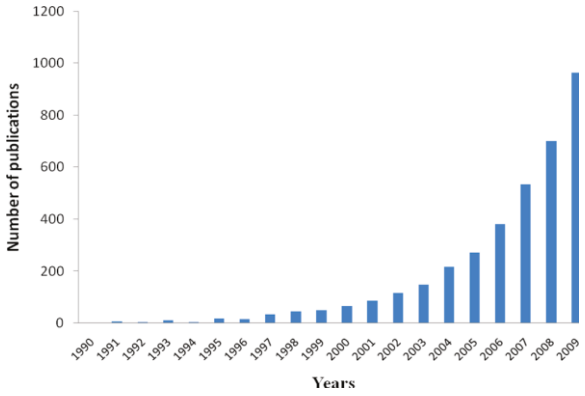

Figure 2: Number of publications featuring the term "metal organic frameworks" in their topics (Source; Keskin and Kızılel, 2011 [20]) *© permission ACS 2018*

2. Nano-Metal organic Frameworks

In the application of MOFs in biological systems, size becomes an important aspect of the particles, since size of a MOF particle will determine its fate in a biological systems [9]. The size of MOF particle therefore poses as a limitation for intravenous administration, thereby necessitating the preparation of monodispersed well defined reproducible and stable nanoparticles for any eventual bio-application [21]. Bulk MOFs often face the challenge of delivering materials of very small sizes; nanoscale MOFs however overcome this barrier as they are able to accomplish the incorporation of such small materials into cells, Sanchez et al [22,23]. Size and shape control can be achieved by judicious choice of synthetic approaches, reaction conditions, stoichiometry of reagents etc. For most bio-applications of MOFs, particle sizes in the range of mesoporous and microporous are desirable owing to their large surface area, pore size, structure stability, high drug loading and their characteristics of bioactivity and biocompatibility, [5, 16-20]. On this note, Gonzalez et al have stated that the pore structure and particle size of nano and mesoporous materials could affect release profile of a hosted molecule in the case of a delivery system. A number of state-of-the-art porous bio- inorganic nanoparticles with microporous and mesoporous sizes, large surface areas, high drug loading and stimuli-responsive drug controlled release property have been reported in literature [9], with their applications suffering serious limitations related to issues of biodegradability and post-functionalisation. Notwithstanding these limitations, tailoring MOFs to meet the challenges of biodegradability post synthetic modification has also been the object of few reports as well as nanoscale fabrication.

3. Current Synthetic Approaches to nanoMOFs

Currently in literature, there are several synthetic methods for MOFs including solvo/hydrothermal, microemulsion, ultrasonic irradiation/sonochemical, mechanochemical, and microwave-assisted synthesis, that have been developed fabricate MOFs. Generally, to obtain nanoscale MOFs, two synthetic approaches (Figure 3) are used;

- Confining the supramolecular assembly; a process that generally leads to MOF formation at nanoscopic locations through methods like emulsions or template synthesis and
- Favouring nucleation against crystal growth, using such methods as fast precipitation or by using microwave and ultrasound synthesis[22].

The synthetic approach employed may yield amorphous or crystalline material depending on the ability to control nucleation and growth kinetics of the nanoparticles [24].

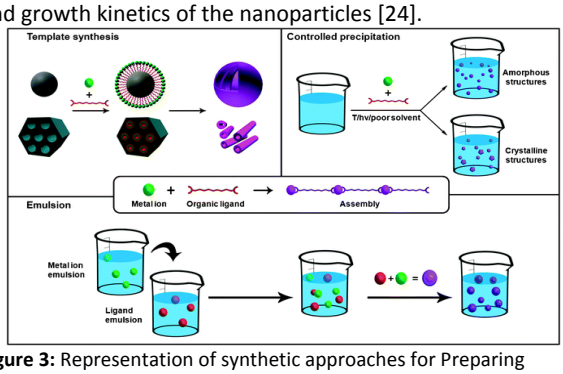

Figure 3: Representation of synthetic approaches for Preparing Nanoscale MOFs [22], [26]. *© permission RSC 2018*

Generally, nanoMOFs particle growth can be achieved by control of either physical parameters such as type of energy supply, reaction time and temperature or chemical reaction parameters such as reactants ratio, addition of modifiers and surfactants [25]; the former approach is however preferred for its convenience.

3.1 Emulsion Methods

As already stated above, this method involves confining reaction zone and controlling shape simultaneously [25]. Additionally, this method also affords control of size and polydispersity of the MOF. Emulsions are formed by suspending small droplets of one solution (stabilized by surfactants) in another, the two solutions however not being miscible. The sizes of the droplets can be reduced to the range 50-1000 nm to obtain nanoemulsion. Nucleation, self-assembly and MOF growth is therefore confined within these droplets which form some sort of nanoreactors. In addition to using the surfactant for stabilization, and size control, Zhao et al have used N-ethylperflourooctysulfonamide (N-EtFOSA) surfactant as template to obtain highly ordered hierarchical micro and mesoporous MOF structure [27]. Yang et al 2014 [28] obtained zeolitic imidazolate framework 8 (ZIF-8) nanospheres via the reversed phase microemulsioin-interfacial synthesis method using polyvinylpyrrolidone, PVP as surfactant to stabilise the zinc acetate aqueous solution in a 1-octanol oil phase.

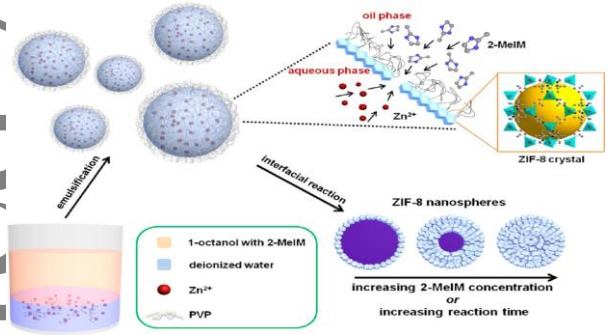

Figure 4: A water-in-oil nanoemulsion using PVP as stabilizer and 1-octanol as the oil phase. Zinc ions in the aqueous phase react with 2-MeIM in 1-octanol at the spherical interfaces of emulsion droplets, to form ZIF-8 nanocrystals which further grow to form nanospheres at room temperature. The shell thickness is controlled by controlling the concentration of 2-MeIM and reaction time [28].

After stirring the oil and aqueous mixture to obtain the inverse emulsion, (water in oil) the reaction was initiated by addition of a solution of 1- octanol solution containing 375 mg of 2-MeIM and shaking gently to initiate the reaction. Transmission electron microscope (TEM) and a scanning electron microscope (SEM) images on the collected nanscale MOFs revealed average diameters 130 nm and a direct correlation between shell thickness and concentration of organic ligands. Reaction time also appeared to show a direct correlation with shell thickness. Rieter et al 2006 [29] obtained Gd based nanorods by suspending aqueous solution of $GdCl_3$ in CTAB/heptane/1-hexanol solution of tri-(methylammonium)benzene-1,2,4-tricarboxylate (1,2,4-BTC) with 10 minutes stirring to obtain a CTAB/isooctane/1-hexanol/water microemulsion system. A further 2 hours vigorous stirring of the resultant mixture led to the formation luminescent nanorods. The same group extended this same method to obtain $Ln(BDC)_{1.5}(H_2O)_2$ nanoMOF (Ln=Eu^{3+}, Gd^{3+}, or Tb^{3+} and BDC=1,4-benzenedicarboxylate) [30]. Seoane et al [31] have recently investigated the effect of pH and H_2O/EtOH ratio on the textural properties of a series of aluminium trimesate MOF prepared in the presence of cationic surfactant cetyltrimethylammonium bromide (CTAB) at 120 °C. NanoMOFs with hierarchical pore size 3-33 nm were formed after 12 hrs in an autoclave maintained at 120 ^{o}C. With a water ethanol molar ratio of 0.6:3.4 and pH of 2.1, the authors found that increasing concentration of the emulsion leads to an increase in the number of nucleation sites which brings about a decrease in particle size but however does not have an impact on the aspect ratio of the nanocrystals. The fact that the nanoparticles did not agglomerate was attributed to the addition of the surfactant which stabilizes the emulsion and constrains the reaction. In a similar development Tian et al [32] prepared gadolinium metal organic framework (GdMOF) nanoparticles using reverse microemulsion and 1-hexanol/heptane mixture as the oil phase using a similar procedure as above. A water to surfactant molar ratio of 10 was used to obtain nanoparticles that were 155 +/- 30 nm in length and 30 +/- 11 nm in width. Cao et al [33] on their part recently obtained ZIF-8 uniform sized nanospheres using sodium dodecyl sulfate as a surfactant. The obtained Zn^{2+}/ 2-methyl-imidazole MOF (ZIF-8) nanosphere showed characteristics of a typical zeolitic imidazolate frameworks (ZIFs) with each zinc ion connected to the 2-methyl-imidazolate by four coordinate bonds giving rise to a hexagonal structure consisting of four-connected zinc ion centres and two-connected 2-methyl-imidazolate. The MOF was successfully used to encapsulate the anticancer 10-Hydroxy Camptothecin (HCPT) as evidenced by the confocal laser scanning microscope (CLSM) using a Leica SP5 for which the fluorescence of HCPT was detected. Zheng et al 2017 [34] investigated on controlled preparation of nanoMOF by ionic liquid microemulsions ionic liquid containing microemulsion system H_2O/BmimPF6/TX-100 to synthesize the thermally stable nanoscale imidazolate framework in the range of 2.3 nm and a narrow distribution less than 0.5 nm. XRD of the synthesized nanoMOFs agree with the molecular simulation and reported literature. The relative small size of these MOFs compared to the La-MOFs has been attributed to the fact that different mechanisms exist for controlling crystal growth for the reaction of the and the metal ions. In order to address the fact that most of the organic starting materials are insoluble or only partially soluble in water, ethanol was added to form a novel ionic liquid microemulsion (ILMEs) with quaternary component so as to improve the dissolution of organic ligands. Unlike conventional emulsion methods, where the MOFs are easily obtained by means of direct centrifugation after the reaction between the ligand and the metal ions, ILMEs are very stable that this method cannot be used to obtain the MOFs that have been formed. The addition of an organic liquid therefore assisted in the collection of the MOFs through demulsification. The limitation of this approach is however remains the fact that the microemuslion cannot be reused owing to contamination of the microemulsion.

3.2 Interfacial Synthesis

Interfacial synthesis relies on the adsorption of metal ions onto porous substrates, followed by the nucleation and growth of MOFs on the surface of porous substrates [35]. Usually one of the precursors (the metal ion or cluster) is adsorbed unto the substrate and used as an interface on which the MOF is grown by allowing the ligand solution to run over the metal containing substrate. The thickness of the MOF can be controlled by controlling the number of metal ions on the substrate while the kinetic control can achieve selective MOF formation [35]. Tsuruoka et al [35] have used this approach to obtain a MOF using metal ion-doped polymer substrate. Continuous densely packed microcrystals MIL-53(Al) were formed after 5 minutes of hydrolysis with the thickness observed to increase with hydrolysis time [35].

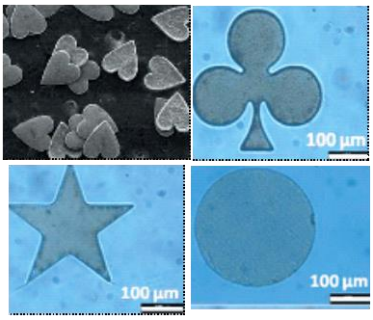

Figure 5: Different Shape obtained using a micrconfiner [36]

Kim et al [36] have fabricated free-standing MOF superstructures having desired shapes by micro-confined interfacial synthesis by using the immiscible liquid–liquid interfacial approach. Shape control was achieved by placing a mold with desired shapes of open windows at the interface of the two liquids. These open window spaces served as microconfiner and localizers of nucleation and growth. High concentration of precursors allowed for the rapid formation of superstructures with shapes varying from rectangle, circle, clover, star, heart, and even characters as dictated by the microcinfiner. Lu and Zhu [37] developed a liquid-liquid coordination mechanism for the synthesis of free standing MOF membranes; the mechanism involves catalysis of the reaction between $Zn(NO_3)_2$ and terephthalic acid dissolved in immiscible liquids using triethylamine as catalyst. At high precursor and low catalyst concentrations membranes were formed, whereas low precursor and high catalyst concentrations produced particulate MOFs precipitated from the DMF phase. SEM and XRD analysis revealed free standing 3D $Zn_4O(BDC)_3$ (MOF-5) and 2D MOF-2 (ZnBDC·DMF) with a sheet-like bottom and particulate top layer.

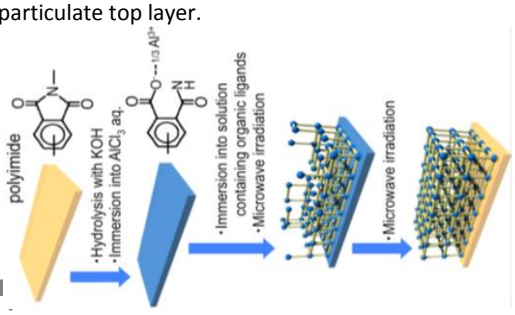

Figure 6: Interfacial synthesis of Al Based MOF on a polymer substrate [35]. *© permission ACS 2018*

3.3 Template Assisted Method

Template assisted technique has also emerged as one of the interesting methods by which nanoMOFs can be synthesized. This technique employs a thin nano supramolecular metal organic film as a growth template unto which the intended MOF is grown by means of deposition technique such as a layer by layer deposition. Usually, at the end of the deposition the thin film can then be removed either by chemical or thermal means. Huang et al [38] recently used this technique to synthesize hierarchical-pore metal-organic frameworks using nanosized Zn based MOF-5 as template on which Zr based MOFs were deposited in a Teflon lined vessel. The acid sensitive templates were removed by stirring in HCl and the resulting MOF showed a mesopore size of about 1 nm smaller than that of the Zn template MOF (370-520 nm) possibly due to decomposition or rearrangement of Zn template MOF particles in the system. The as-synthesized MOFs showed good porosity and potential applications, such as in large molecule adsorption and the mesopore sizes of the MOFs can be tuned by varying the concentration of templates. Liu and co-workers [39] have posited that the template assisted technique is a potential approach to obtaining interesting MOFs whose synthesis might be difficult to obtain via routine synthetic routes. In other to investigate the influence of organic molecules bearing reactive functional groups as templates on the structures of the resulting MOFs they synthesized four novel complexes based on the pyridyl carboxylic acid ligand 5-(pyridin-4-yl)isophthalic acid (H_2pyip); $[Mn_3(pyip)_2(HCOO)_2(H_2O)_2]_n$ (**1**), $\{[Co(pyip)(H_2O)]\cdot H_2O\}_n$ (**2**), $\{[Mn_2(pyip)_2(H_2O)_4]\cdot 5H_2O\}_n$ (**3**), and $[Co(pyip)\text{-}(EtOH)(H_2O)]_n$ (**4**), under solvothermal conditions. **1** was obtained as a 3D coordinated framework using a 4, 4'-bipyridyl template while a 2D framework was obtained for **2** using cyanoacetic acid as the template. **3** and **4** were obtained without templating agents with **3** showing an infinite 2D network with a 1D penetrating water chain resulting to a 3D supermolecule while **4** contains two independent 2D networks further connected to a 2D double-layered supramolecular framework by hydrogen bonds. The efficiency of template assisted synthesis depends of the strong interaction that exists between precursors and the template as it helps in directing the growth of the MOF. Weak interactions or the absence thereof leads to segregation consequently undermining desired directed approach. In view of this, Sun et al 2012 [40] developed a cooperative template system consisting of a surfactant (cetyltrimethylammonium bromide) and a chelating agent (citric acid) to fabricate a series of mesoMOFs with hierarchical mesopores interconnected with micropores. The citric acid was used to create an interaction between the metal ions and surfactant molecules by means of electrostatic Coulombic interactions. While the surfactant is used as a template, immobilizing the citric acid on the surfactant also renders it to sever as a co-template unto which the Cu ions are directed.

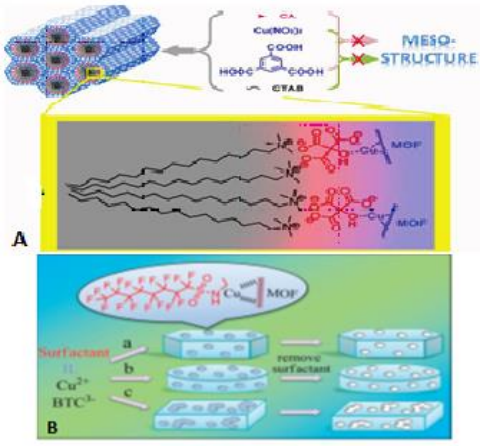

Figure 7: A: Use of citric acid to create interaction between Cu ions and surfactant molecules [40]. **B** Using N-ethyl perfluorooctylsulfonamide to direct particle growth [41]

The mesoporous MOF obtained under solvothermal conditions showed well defined mesostructure with crystalline microporous framework and the amount of mesopores can be varied by varying surfactant/chelating agent ratio. The authors have importantly noted that the addition of CTAB alone does not lead to the formation of mesoporous material unlike in the case of mesoporous oxide synthesis indicating that CTAB alone cannot be used as template for directing MOF synthesis. Peng et al [41] reported on a surfactant assisted mesoporous MOF synthesis where the surfactant played the dual role of both directing the particle growth and templating. The surfactant, N-ethyl perfluorooctylsulfonamide directs the particle growth by selectively adsorbing unto the crystallographic planes of the MOFs.

3.4 Irradiation Assisted Methods

As already noted above, one approach to obtaining nanoMOFs is by preventing extensive nabbing particle growth. In solvothermal synthesis, irradiation with microwave or ultrasound is capable of obtaining fast precipitation and nucleation which leads to the formation of nanosized particles. The use of ultrasound emanate from acoustic cavities which generate local hot spots with high temperatures of about 500 K, pressures greater than 1000 atmospheres and rapid heating/cooling rates of about 10^{10} Ks^{-1} occurring in milliseconds [25]. These hot spots serve as nucleation sites thereby limiting extensive particle growth so that the resulting particles are likely in the nanosize range. Following a pioneering work in synthesis of MOFs using this technique by Qiu and co-workers [42], several reports have emerged on this technique. In the case of microwave assisted technique localized heating derives from the fact that polar solvents possess high dielectric absorptivities which results to rapid thermal energy conversion and excellent local heating [2]. This results to situations similar to that occurring to ultrasound irradiation where the local hot spots serve as nucleation centres for particle growth. Both methods have characteristics of high efficiency, exhibit phase selectivity, suitable for obtaining small sized particles, and offers possibility for exercising control of the morphology of the materials [2]. In addition to the above advantages, sonochemical and microwave assisted techniques considerably shorten reaction time compared to conventional heating method. The microwave approach for MOF synthesis was first reported by Choi et al [43] in 2006 to obtain for the first time MOF-5 denoted MW MOF-5 at at 27% yield within 9 minutes of microwave irradiation with morphology similar to previous reports and length 2-4 nm. This success prompted further investigation leading to a large number of papers published in literature on this synthetic approach. Lin et al [44] proved the efficacy of this approach by reducing the synthesis time for a series of isostructural microporous 3D lanthanide MOFs from three days under solvothermal conditions to within few minutes using microwave irradiation at same temperature and yield. This is proof of the efficacy of MW assisted synthesis. The similarity in size of obtained particles, reduction in reaction time and energy consumed all make this method attractive for upscale synthesis of MOFs. In a similar development, Bag et al [45] have used microwave assisted synthesis for the large scale synthesis of a series lanthanide metal–organic frameworks (Ln-MOFs), possessing preferred conformation and photoluminescence properties. Microwave irradiation of the reaction mixture for 5 minutes gave yields greater than 60% for all the MOFs synthesized. Similar reports by Taylor-Pashow et al [46] have equally obtained highly crystalline Fe(III)-carboxylate nanoscale metal-organic frameworks (NMOFs) with the MIL-101 with diameter approximately 200 nm in modest yields (20%) for drug loading and delivery.

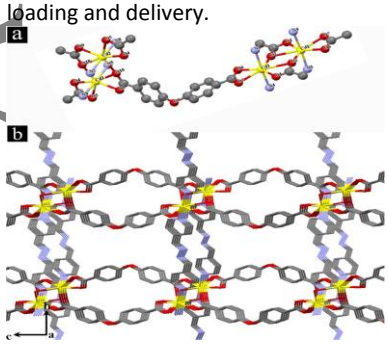

Figure 8: Representation of channels along a-axis of TMU-8(left) and TMU-9 (right) [47]

Masoomi and Morsali [47] obtained nanoplates of two Cd(II) based MOFs $[Cd_2(oba)_2(4\text{-bpdb})_2]_n$ $(DMF)_x$ (TMU-8) and $[Cd(oba)(4,40\text{-bipy})]_n \cdot (DMF)_y$ (TMU-9) in an ultrasonic bath at ambient temperature and atmospheric pressure. The 3D nanoplates form with relative ease upon sonication with morphology similar to that obtained from simulation and IR data similar to that obtained via conventional heating method indicating the efficacy of the method. The 3D network of TMU-8 arises from 2D sheets connected through a linear 4-bpdb and two channels along a-axis occupied by DMF guest molecules. TMU-9 on the other hand contains narrow channels along a- and b-axes. Longer sonication time yielded thinner sheets while high concentrations led to the formation of thicker MOFs nanosheets. Ultrasound-assisted synthesis of nano-structured 3D $[Zn_2(btec)(DMF)_2]_n$ (**1**) (btec = 1,2,4,5-benzenetetracarboxylate) metal–organic polymer has been reported. Rod-like nano-structure compound is obtained by reducing the concentration of the initial reactants. Although high ultrasound irradiation produces plate-like morphology [47] it also leads to products with non-uniform morphology [48]. Bigdeli and Morsali [49] in a similar direction synthesized a mixed ligand nano-structured zinc(II) amidic rods $\{[Zn_4(BDC)_4(bpta)_4]\cdot 5DMF\cdot 3H_2O\}_n$ (1) (bpta=N,N'-bis(4-pyridinyl)-1,4-benzenedicarboxamide, BDC=1,4-dicarboxylate) MOF using solvothermal-ultrasonic irradiation at ambient temperature. The similarity in XRD patterns for simulated, hydrothermal and sonochemical obtained MOFs indicated that the nano-structured compound obtained by the sonochemical process is identical to that obtained hydrothermal synthesis. Smaller particle sizes (nano-rods) are obtained by imposing high initial concentration, high ultrasound power and shorter sonication times. These results however seem to contrast reports by Masoomi and Morsali who have posited that lower concentrations will yield reduced particle size although both report agree on the effect of ultrasound power. Most recently following success of their previous work, Begdeli et al [50] obtained MOFs as precursors for ZnO nanostructures. 3D nano porous Zn(II)-based MOF $\{[Zn_2(oba)_2(4\text{-bpmn})]\cdot(DMF)_{1.5}\}_n$ (TMU-21), (4-bpmn=N,N'-Bis-pyridin-4-ylmethylene-naphtalene-1,5-diamine, H_2oba = 4,4'-oxybis(benzoic acid)) was obtained within few minutes of sonication. Morphology and size can be varied factors as in their previous work [49]. As an addition, compounds (TMU-21) and $\{[Zn_2(oba)_2(4\text{-bpmb})]$ (TMU-6) reported in their earlier work were prepared by mechanochemical synthesis. Haque et al [51] obtained MIL-53(Fe) MOF by solvothermal method using conventional electric, ultrasound irradiation and microwave in an attempt to understand accelerated synthesis by ultrasound and microwave irradiation. While no visible change with reaction temperature or time is observed for MIL53(Fe) synthesized by the three methods as revealed by the SEM images, morphology showed dependence on synthetic method with US and MW producing homogenous nano particles as opposed to conventional electric heating.

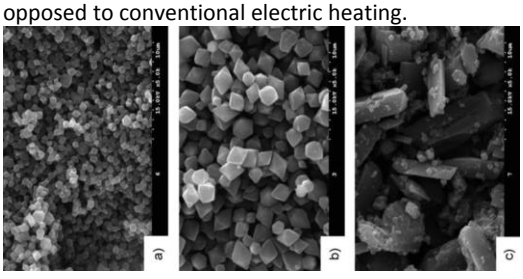

Figure 9: SEM images of fully crystallized MIL-53(Fe) synthesized at 70 °C by a) US for 35 min, b) MW for 2 h, and c) CE for 3 d [51].

The rate of synthesis for the three methods has been found to decrease in order US>MW>>CE. Pardakhty and Ranjbar [51] used ultrasound to obtain uniform crystals of average size 3–12 µm within 20 minutes of ultrasound irradiation. Pursuant to report by Masoomi and Morsali on the effect of US on morphology and

size, Ata-ur-Rehman et al [52] recently obtained MOF-5@MWCNTs using a combination of both sonication and microwave irradiation. Drop-wise addition of the metal precursor to the ligand under sonication at 60 ^{o}C and subsequent microwave irradiation during 30 minutes led to the formation of cubic uniform sized MOF-5 nanoparticles of high BET surface area and large pore volume.

3.5 Spray-Drying

This is a technique widely used to convert a liquid product into a dry powder in a single step. Spray drying has been used in several areas such as miniaturisation [53], drying, encapsulation [54], [55] and synthesis of materials [22]. Unlike the emulsion methods for MOF synthesis, this approach does not require any secondary immiscible solvents or surfactants and equally escapes other factors such as temperature, solvents, bases solubility which render synthesis sometimes challenging [23]. It equally offers the possibility of obtaining multicomponent MOF superstructures and encapsulation of guest molecules within the structures. The principle behind this approach involves fast drying of aerosol dispersion containing micro-droplets of the precursors [22] using a hot gas [56]. Precipitation within the droplets sprayed on a surface is initiated by evaporation in the droplets with the droplets serving as a confinement for the reaction and growth. The sizes of the MOF crystal can be controlled by controlling the sizes of the droplets. During the evaporation process, the droplet shrinks and reaches a critical concentration at which point the nanoMOFs begin to form at the surface; confined to the surface of the droplet, the MOF particles finally merge into a well packed shell [23]. Although spray – drying is less commonly used amongst precursor laboratory techniques such as sol-gel or co-precipitation, it present substantial advantages such as reproducibility and scalability reason for its wide application in the industry [57]. Garzón-Tovar et al [58] have reported on spray-drying continuous-flow method for simultaneous synthesis and shaping of microspherical high nuclearity MOF beads in which spray-drying and continuous flow were used for the continuous synthesis of MOFs. The process involves the continuous injections of precursors into a heating coil connected to the nozzle of the spray-dryer where they are heated to initiate nucleation from where they are injected into the spray-dryer at the same feed rate. Within the spray-dryer, the MOF precursors are atomised into a spray of microdroplets. Field-emission scanning electron microscopy (FESEM) and PXRD of the synthesized UiO-66 revealed highly compacted homogenous spherical solid beads with average diameter of 4.3±2.6 µm.

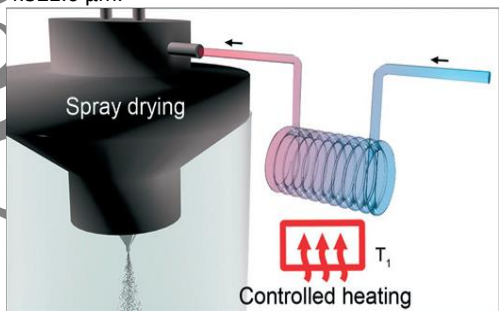

Figure 10: Heating coil connected to the nozzle of the spray-dryer [58]. *© permission RSC 2018*

The combination of spray-drying and continuous flow was proven to work in synergy for optimal yield and quality of the material as spray drying alone yielded amorphous solid while continuous flow alone gave products much lower yield and quality. The generality of this approach for high nuclearity was proven by synthesis of other analogues such as UiO-66-NH_2, UiO-66-NO_2, UiO-66-Br, UiO-66-$(OH)_2$ etc. Guillerm et al [59] synthesized porous M-XF6-based metal organic and hydrogen frameworks (M= Cu, Co, and Zn) with high crystallinity and purity. The nanosize range (3.5 ±2.7 – 7.9±4.8 µm) and homogenous nature of the spherical superstructures was revealed by FESEM and PXRD. TEM analysis revealed a crystal size of 32±13 nm for SIFSIX-3-Co, 80±12 nm for SIFSIX-3-Cu and 28±9 nm for SIFSIX-3-Zn. Carne-Sanchez [23] obtained nanoscale HKUST-1 MOFs from hollow superstructures synthesized by means of spray drying at a yield of 70% and 90% purity. FESEM confirmed the hollow spherical superstructures with diameter 2.5±0.5 µm and thin uniform walls made up of packed octahedral nanoparticles which showed considerable stability to mechanical stirring and solvent but disintegrated upon sonication to yield nano particulate MOFs.

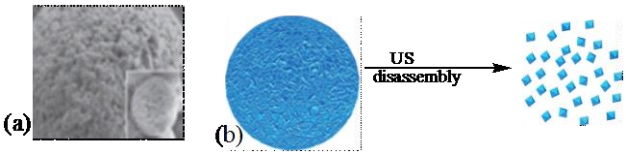

Figure 11: (a) shows the FESEM spherical hollow superstructure of KHUST-1 while (b) show a scheme to obtain the nano KHUST from disassembly of (a)

Earlier on KHUST-1, ZIF-8 and $Fe_3(BTC)_2$ were obtained in a one-pot synthesis through spray drying and Evaporation Self-induced Assembly (ESIA) using templates in some cases. While nanoparticles of KHUST-1 and $Fe_3(BTC)_2$ were obtained after activation, ZIF-8 nanoparticles obtained small crystalline spherical structures of about 100 nm [60].

3.6 Mechanochemical Synthesis

One of the greatest challenges MOFs have faced is that of maintaining the porous framework structure once the solvent is removed. The collapse of the framework upon removal of solvent usually renders the MOFs non-applicable as most of their applications are dependent on their porosity. In light of this challenge, solvent free mechanochemical synthesis approach involving solid-solid reaction has become an ideal approach to structures which are likely to collapse upon removal of solvent molecule form the pores. This method basically relies on grinding precursor solids together using automated ball mills so as to cause them to react without solvent or minimal amount of solvent [56]. Advantages of this method over others is that the yields are quantitative and in powdered form ready for application thereby avoiding time consuming treatments and issues of solubility [61]. Purification which may require a solvent and scalability however, remain main setbacks of this approach. The mechanochemical synthetic approach can yield 1D, 2D and 3D products [62]. Three main approaches have been employed for mechnochemical synthesis;

- Liquid assisted grinding [63] wherein the liquid is used in minimum amount to assist mobility and catalysis of the reaction,
- Ion-and-liquid assisted grinding where the liquid serves the same purpose in liquid assisted grinding and small amounts of a salt is employed to hasten MOF formation [56] and
- Solvent free grinding [56].

In this light, Yousefi and Zeid obtained a copper based nanoMOF $Cu_3(BTC)_2$ by ball milling the precursors through the liquid

assisted grinding. The change in color of the powder indicated the occurrence of a reaction and the XRD pattern of the obtained nanoMOFs was consistent with reported literature [63].

3.7 2D nanostructure Synthesis

Research in 2D thin sheet MOFs has spiked recently due to the number of complementary schemes that have been designed for synthesis and the fact that they can be tailored to meet specific applications [25]. Various patterns have been designed for this purpose including direct oriented or non-oriented growth from preconditioned solvothermal mother liquors, electrochemical growth, deposition from colloidal MOF suspension, deposition based on sol-gel approach, stepwise deposition and top-down approach. We shall however discus only a few of the approaches here.

3.7.1 Top-down Approach

This method involves deconstruction or delamination of a bulk MOF to nano particles. The deconstruction could be done via ultrasound, or other methods. This method operates on the principle that within a crystalline bulk, there exist layers held by physical interactions such as Van Der Waal forces or H-bonds. Eventual destruction of these interactions can lead to exfoliation of the layers which can be suspended in solvents and ultimately isolated. For this reason this method is ideal for obtaining 2D MOFs as most reports have so far dealt with 2D nanoMOFs sheets. This method is however relatively new and few reports have surfaced on this approach, research on this method would definitely prove useful. Razaei et al [64] have recently used this approach to obtain nanoMIL-100(Fe) by first obtaining the bulk MIL-100(Fe) MOF via hydrothermal synthesis followed by deconstruction using ultrasound irradiation. Peng et al [65] obtained 2D nanosheets of $Zn_2(bim)_4$ from the bulk material by using a combination of wet ball milling and sonication. The wet ball milling assisted the penetration of methanol into the interlayer spaces so as to weaken the interactions while the sonication that followed in n-propanol led to exfoliation and eventual stabilization of the sheets by the propanol by means of adsorption. Foster et al [66] synthesized Cu and Zn based MOFs via hydrothermal synthesis. Nano sheets of thickness 3-30 nm were obtained by deconstructing the obtained MOFs via sonication; adding alkyl layers to the solution prior to deconstruction aids in the dispersion of the sheets in the aqueous solution. It was also observed that concentrating the sonicated solution leads to restacking which appears to be a major drawback of this technique despite the relative success [67]; obtaining stable sheets therefore remains a challenge that demand further research.

3.7.2 Gel Layer Approach

Unlike other approaches that are capable of achieving oriented growth, this approach generally does not. This method however, allows facile control of MOF thickness by means of concentration and procedures. It has a few advantages with regards to the fabrication of MOF films such as needing no pre-treatment of substrates and solvents during crystallization, good compatibility between substrate and MOF layers, possibility of reusing MOF precursors, relative ease of manipulating the position of MOF layer, and time-effective processes. Li et al [68] prepared ultrathin MOF by depositing a Zn based gel on ammoniated polyvinylidene (PVDE) hollow fibres. Heat treatment of the gel coated fibres transformed the gel to intergrown nanosized crystals.

3.7.3 Layer by Layer Growth

This technique involves the step by step growth of surface immobilized MOFs commonly referred to as SURMOFs. The technique involves cyclic immersion of a substrate (usually functionalised) into precursor solutions and allowing them to react. Variations to this in include exposure to metal/ligand solutions in flow reactors and through spray deposition [69].

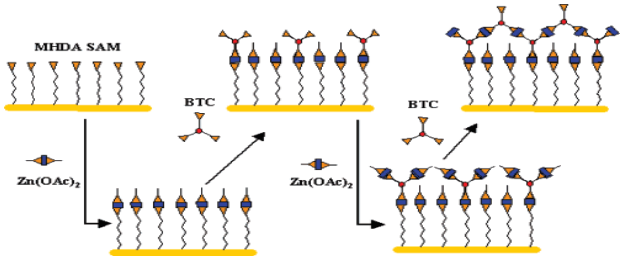

Figure 12: Representation of the layer-by-layer growth of the metal-organic polymer on the 16-mercaptohexadecanoic acid MHDA self-assembly monolayer SAM obtained by repeated immersion cycles for 60 minutes in solutions of $Zn(CH_3CO_2)_2$, ($Zn\text{-}(OAc)_2$), and then BTC [70]. *© permission ACS 2018*

This technique represents an alternative approach of growing SURMOFs heterostructures with possible improved morphology [69]. Unlike bulk MOFs SURMOFs present highly oriented structure, homogeneous morphology with a smooth surface, facile control of thickness through deposition cycles and limited defects MOF [71]. Initially introduced by Shekhah in 2007 [70] to synthesize a Zn benzene tricarboxylate MOF, this method can be used to control both orientation and number of MOF layers grown on a surface. The MOF layer is grown by dipping the growth substrate into precursor solutions repeatedly with the number of cycles corresponding to the number of MOF layers. The thickness of a film can therefore be controlled by number of the functionalized precursor is dipped into the other solution. Shekhah later further investigated the growth of different MOFs on substrates functionalized with COOH, OH, and pyridine obtaining highly oriented grown and homogeneous films [72]. In another study the same group investigated the liquid-phase epitaxy (LPE) of HKUST-1 for different carboxylic terminated templating organic surfaces prepared via self-assembled monolayers SAM, on Au substrates. The obtained SURMOFs showed excellent oriented growth along the crystallographic direction (100) when 16-mercaptohexadecanoic acid MHDA, was used while use of 9-carboxy-10-(mercaptomethyl)triptycene CMMT result to the growth in the direction (111) and 4'-carboxyterphenyl-4-methanethiol TPMTA yielded film deemed inferior [73].

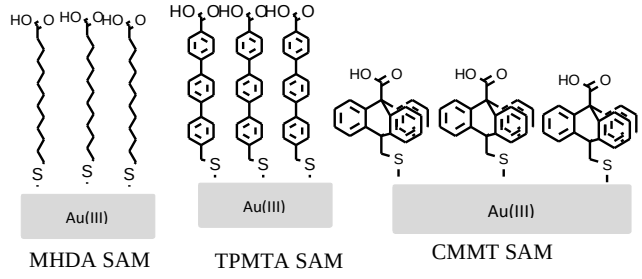

Figure 13: Carboxylic groups-terminated self-assembled monolayers (SAMs) on Au substrate. [70], [72]

Summerfield et al [69] showed that it possible to grow more than a single layer per cycle of dipping the substrate into precursor solution. They obtained HKUST-1 films on Au(111) in which the crsytallites are capable of growing 5-10 layers per cycle as

revealed by atomic force microscopy. Interestingly, they found that despite reports that on bare Au surface (absence of thiol SAMs) functionalities MOF growth is not possible [15], it is possible to obtain MOF on a bare Au(111) surface. Multi-layer surface induced thin film MOF assembly from Co^{2+} ion and deprotonated free-base porphyrin (H_2TCPP^{4-}) using the sequential coordination from the amine-modified surface substrate has been reported by Laokroekkiat et al [71].

4. Functionalization of MOFs

The applicability of MOFs depends to a large extend on their functionalities since several of the applications rely on the possibility of incorporating various functional groups into the MOFs. Two approaches could be used to introduce the functionalities in MOFs; either functionalizing the ligand prior to synthesis of the MOFs or functionalizing the MOF after synthesis usually referred to as post synthetic modification, PSM. Serious challenges including linker solubility, thermal and chemical stability, and functional group compatibility are inherent with the [2] modification during synthesis; a situation that can be tackled using the latter approach. Several PSM protocols are reported in literature including covalent transformation of pendant and integral functional group, surface modification, Post-Synthetic Deprotection (PSD), metalation, linker exchange, and inorganic cluster modification. The success of any functionalization approach lies in its ability retain the underlying structural integrity of the MOF while improving on it functionality.

Since the incorporation of functional groups into MOFs can enhance their functionality, much focus in research has been driven toward obtaining MOFs with functional groups poised to improve functionality. This for the most cases has been achieved through using ligands with desired functional groups. The above mentioned complications arising from the presence of functional groups has however also been a limitation to achieving desired objective. Resorting to post synthetic modifications has therefore been a major focus in obtaining functionalized MOFs. The success of this alternative method has prompted further research as evidenced by the considerable number of publications witnessed on the subject [10,74]. PSM has so far mainly been via modification of organic linker through chemical reactions [2] or through electrostatic interactions that do not compromise the integrity of the resulting structure even though there are also reports involving the modification of inorganic component. Here, we examine some of the commonly employed PSM protocols.

4.1 Pendant Covalent Functionalization

The transformation of pendant functional groups in MOFs is an interesting approach to functionalizing MOFs. In this approach, the organic ligand is covalently modified after the synthesis of the MOF has been completed. Most reports on transformation of pendant functional groups have thus far majored on the transformation of pendant amino groups possibly due to their wealth of chemistry [75]. Hintz and Wuttke [75] carried out PSM on MIL-101(Al)-NH_2 by transforming the pendant NH_2 with acetic acid using *N,N´*-diisopropylcarbodiimide (DIC), *N,N,N´,N´*-tetramethyl-O-(1H-benzotriazol-1-yl)uronium hexafluorophosphate HBTU, bromotripyrrolidinophosphonium hexafluorophosphate PyBroPs, and 1,1´-carbonyldiimidazole CDI using dichloromethane and DMF as solvents. High yields were obtained for dichloromethane and the author suggested solvation effect as possible reason for high yields indicating that the success of PSM does not only depend on the coupling agent used but as well the solvent in which the PSM is carried out. The authors also investigated the coupling with glycine and well known analgesic acetylsalicylic obtaining yields 41.8% and 6.4% respectively. The low yield of acetylsalicylic was ascribed to low reactivity of aromatic acid.

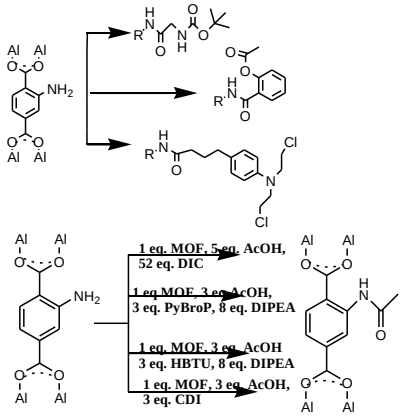

Figure 14: Transformation of pendant NH_2 by reaction with various reagents [76].

Molavi et al [77] recently modified the NH_2 of NH_2-UiO-66(Zr) with glycidyl methacrylate via ring opening reaction between the NH_2 of the MOF and the epoxy group of the methacrylate obtaining a functionalised crystalline MOF whose morphology and stabilibilty remained unchanged compared to the unfunctionalised material despite small decrease in pore volume and size of the functionalized MOF. Similar reports by Zhang et al [78], Morris et al [79], Tanabe et al [80] have also achieved success in functionalizing MOFs by means of NH_2 transformation converting the NH_2 to $-N_3$, $-NH_3^+Cl^-$ and ketone respectively. Yang et al [81] on the other hand obtained alkali and acid stable MIL-101(Cr) grafted pyridine after refluxing a mixture of MIL-101(Cr) and pyridine for 24 hours. Functionalizing the MIL-101(Cr) did not lead to any significant change in the morphology of the MIL-101(Cr) but played an important role in the high performance separation of tocopherols. Furthermore, Yang et al [82] synthesized a folate-targeted zinc-based nanoMOFs (FA-IRMOF-3) via post-synthetic modification and tested their performance as a targeted drug carrier in vitro. The PSM was carried out by conjugating the tumor targeting folate to the pendant NH_2 group in the MOF linker. Drug loading experiments revealed 24% loading capacity of 5-floururacil and the MOF structure uncompromised. The drug-loaded nanoMOFs showed improved cytotoxicity compared to the free 5-flourouracil against three cancer cell lines *in vitro* with a distinct selectivity between folate receptors positive and negative cells. Koppen et al [83] have recently obtained a series of bismuth based MOFs and functionalized using different reagents attached to the pendant NH_2 group with the length of the R- group appearing to affect the yield.

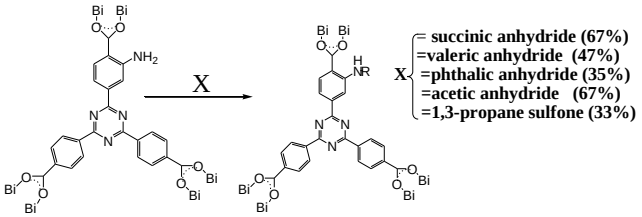

Figure 15: PSM by reaction of different groups with NH_2 with per cent yields indicated in brackets.

While succinic and acetic anhydride produced relatively high yields, larger valeric, phthalic and 1,3-propane sulfone gave relatively low yields owing to the steric hindrance. In the case of

1,3-propane sulfone, an ammonium salt was produced unlike the amides for the other reagents.

4.2 Integral Covalent Functionalization

Consequent upon the fact that most of the linkers in a MOF are generally less reactive, integral functionalization is less common compared to pendant functionalization since it usually involves introducing a functional group unto a linker structure within a MOF. Introduction of functional groups is highly dependent on stability of the MOF structure. This approach to functionalization is possible for high stability MOFs capable of withstanding harsh reaction conditions. In the case where the linker moiety contains aromatic ring, such harsh conditions can favour the introduction through electrophilic substitution reaction mechanism of functional groups such as -OH, $-NH_2$, -X (X = Cl, Br, I), $-NO_2$, $-SO_3H$, alkyl chain, RCHO- etc unto the aromatic ring. Depending on the desired functional group, the introduced functional group can further be transformed. In this regard, the high thermal, photo and solvent stability of UiO-66 MOF family has been reported [84]. Haven been unsuccessful synthesizing UiO-66-OH, Aguilera-Sigalat et al [85] have taken advantage of the high stability of the parent MOF in many reaction environments to obtain UiO-66 by introduction of OH unto the aromatic ring while leaving the structural integrity of the framework unaffected. The conversion of UiO-66 to UiO-66-OH is achieved by exposing the parent MOF to UV in the presence of magnetic TiO_2 as catalyst. In a similar development, DeCoste et al [86] obtained a chlorinated aromatic ring by exposing UiO-66-NH_2 to a stream of Cl_2 gas with the Chlorine substituting at the ortho position via electrophilic aromatic substitution mechanism, Figure below.

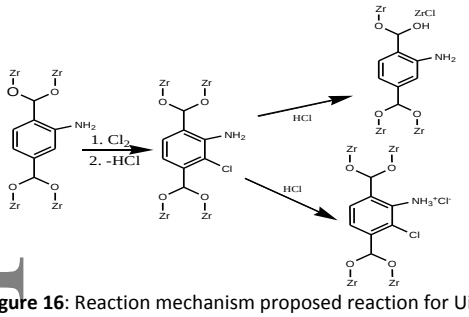

Figure 16: Reaction mechanism proposed reaction for UiO-66-NH_2 with Cl_2

Beyond introduction of functional groups to aromatic rings, Xu et al [87] have functionalized UiO-67-bpy to obtain UiO-67-bpy-Me by *N*-quarternization of the pyridine sites by treatment of the parent MOF with iodomethane to achieve methylation. The occurrence of ^{1}HNMR peaks at 4.21 and 4.33 ppm in the functionalized product corresponding to N-methyl and *N*-methylpyridinium confirmed the methylation. UiO-67-bpy-Me showed lower thermal and chemical stability, as well surface area compared to parent framework, it showed enhanced CO_2 uptake compared to the parent MOF. Zhang et al [88] have successfully achieved similar functionalization at pyridine sites of the bipyridine linker of Zr-MOF. Marshall et al [89] have functionalized Zr and Hf based MOFs by means of stereoselective halogenation of integral alkenes, alkynes and butadiene using N-bromosuccinamide as brominating agent a continuation of earlier works [90], [79-80] in which the neat bromine was deemed too harsh for the MOF. The retention of crystal structure indicated the stability of structure upon functionalization.

4.3 Post synthetic Exchange (PSE)

As the name suggest, post synthetic exchange involves exchange of either the inorganic or organic constituents of the framework after synthesis. The purpose of the exchange (which might either be done in a controlled manner of completely) is usually to reveal functionalities which otherwise cannot be obtained during synthesis [92]. The application of this method can generate entirely new MOFs or MOFs with chemical functionalities that would otherwise not be possible through synthesis. Additionally, this method offers the possibility of control over size and shape of a pores, catenation, and access topologies that are unknown for a particular linker/node combination [93–95]. Post synthetic exchange could either take place in solvent-mediated solid-solid reactions, as well as under solid-liquid conditions [93]. Since the initial reports by Burnett et al [96] proving this concept in 3D MOFs, the idea has grown to almost all sorts of MOFs. The selective exchange of pillar ligands of SALEM-5 (L1, 9 Å) with L3, L4, and L5 (11, 14, and 17 Å), respectively resulted in the tuning of porosity and pore aperture of the SALEM-5 [97] without altering the structural and morphological integrity of the framework. Smith et al [93] carried out PSE in UiO-66 obtaining transmetalated heterometallic Ti_5-UiO-66 and Zr_5-UiO-66 with higher BET surface areas (1011 m^2/g and 965 m^2/g, respectively) compared to that of the "solvent-only" exchanged MOFs, (with surface areas in the range of 800–900 m^2/g) in which self-exchange occurred between terephthalic and benzoate linkers. A similar report whereby Zr in UiO-66 is exchanged with Ti has been reported by Lau et al [98] in which they found that the amount of Ti in the modified UiO-66 is directly proportional to the incubation time. Replacing Zr with Ti leads to decreased in pore size to the range of CO_2 due to the small size of Ti compared to Zr. The modified MOF showed enhanced CO_2 adsorption capacity compared to parent MOF as a result of higher BET surface area [93], decrease in pore size within MOFs which delivers more effective potential energy well-overlap between adsorbent surfaces. Charge transfer from the metal to the ligand by replacing Zr(IV) with Ti(IV) leads to an increase in CO_2 enthalpy and uptake. Recently an alternative method in which no linker is added has developed referred to as post synthetic annealing wherein linkers already incorporated within the MOF (in which there is more than one linker) exchange with one another leading to alteration in the MOF's properties; this is however different from the thermal assisted annealing (such as reported by Gadipelli and Guo [95]) whereby partial decomposition of MOF is obtained by heating [93]. While this technique is still new and warrants further investigation, it presents an interesting approach owing to the fact that no reagents are introduce into the as-synthesized MOFs. Smith et al [93] showed prove of this concept by achieving solvent only modification of UiO-66 to form PSA*x*UiO-66 (PSA*x* = post synthetic annealing in days), in which UiO-66's labile terephthalic and benzoate linker species "self-exchange" resulting in a benzoate-rich crystal surface. Diffraction patterns for the PSA*x*UiO-66 were identical to UiO-66 indicating retention in the structural integrity of the MOF. Fei ei al [99] reported on solid-liquid assisted postsynthetic metal ion and ligand exchange in zeolitic imidazolate frameworks (ZIFs) wherein they achieved partial replacement of Zn in Zn(II)-based ZIFs with radioactive Mn(II) and 4,5-dichloroimidazole with bromoimidazole. The investigation involved stepwise introduction of metal ion followed by ligand introduction then by metal ion. Reversing the order of introduction to ligand-metal-ligand gave product similar as the former indicating that the composition of the product was independent of sequence of introduction followed. Jiang et al [100] improved the Lewis acid-base interactions of a benzotriazole-containing zeolitic imidazolate framework via post synthetic ligand exchange. ZIF-7-M MOF which could not be obtained by means of direct synthesis was successfully obtained by PSE of the benzoimidazole in ZIF-7 with benzotriazole in methanolic solution. The PSE is affected by such factors as solvent, time, temperature, and concentration of

benzotriazole. Fluch et al [101] recently carried out PSE of benzenedicarboxylate (bdc) by similar sized 2-iodobenzenedicarboxylate (I-bdc) in UiO-66 MOF and for first time confirmed the success of the process using non-invasive Rutherford backscattering spectrometry (RBS) that has typically been used in the study of near surface composition of materials particularly thin films. The elastic scattering of a beam of particles by the Coulomb potential of the material enabled not only confirmation that PSE had occurred but as well the quantification. This non-destructive quantification method to determine the yield of PSE reactions in a metal–organic framework is very attractive as it could give insight into the elucidation and kinetics of controlled exchange. Szilágyi et al [102] introduced defects in a MOF material by carrying out PSE in order to enhance CH_4 uptake. Linker vacancy and dislocations were created by exchanging the bdc linker with NH_2-bdc linker in well-known MIL-101 MOF and their presence confirmed by PXRD, IR and TGA. While the defects served as adsorption pockets for methane, H_2 adsorption has been shown to take place at the NH_2 functional group of the NH_2-bdc. Boissonnault et al [103] recently investigated the PSE in MOF-5 UMCM-8, and UiO-66 MOFs. After an 18 hrs exposure of MOF-5 to benzene-2,3,5,6-d_4-1,4-dicarboxylic acid (H_2BDC-d_4) in THF, a core-shell architecture where incorporation of BDC-d_4 occurs at the surface and extends inward toward the center of the crystal with an exchange depth of ~80 µm was observed. The concentration of the BDC-d_4 is found to decrease toward the center of the crystals for all the MOFs and is unaffected by the concentration of the BDC-d_4 in solution or the solvent used. The concentration gradient has been explained by the fact that whereas the carboxylic acid diffuses slowly into the pores of the MOFs, exchange takes place faster compared to the diffusion.

4.4 Surface Functionalization

This technique has to do with confining post-synthetic modification to the surface of a MOF and is particularly attractive for drug delivery [92]. Many of the first reports limiting PSM to the surface focused on stabilizing MOF nanoparticles for drug delivery [104]. Surface functionalization of MOFs used as delivery vehicles is essential because it increase stability, afford good release kinetics, offers the possibility of controlling particle internalization [105]. By carrying out surface modification, it is possible to play around with hydrophilicity and hydrophobicity; properties that are paramount to the application of MOF for drug delivery but without any alteration to the internal porous nature. Surface modification can be achieved through three main approaches namely; coating the MOF surfaces with polymers or silica, carrying out coordinative ligand or metal exchange and covalent surface modification. It has been reported that beyond maintaining a favorable drug release profile, coating a MOF with silica offers possibility of introducing additional functionalities by grafting a silyl-derived molecule onto the silica shell through surface silanol groups to impart additional functionality [106]. Coating a MOF with silica shell has several benefits such as improved water dispersibility, biocompatibility, and the capacity to further functionalize the core-shell nanostructures by means of co-condensation reactions of siloxy-derived molecules. One major advantage of surface functionalization especially with organic molecules is that pendant functional groups on the organic linker on the surface of MOFs can be activated and used to introduce other compounds onto MOFs [107]. Rieter et al successfully coated the surface of a series of $Ln(bdc)_{1.5}(H_2O)_2$, (where $Ln=Eu^{3+}$, Gd^{3+}, or Tb^{3+}) MOFs with silica. The MOF surface was initially coated with hydrophilic polymer polyvinylpyrrolidone (PVP) to prevent agglomeration and protect the MOF against hydrolysis prior to deposition of variable thickness of silica coating using tetraethyl orthosilicate, TEOS. TEM and TGA were used to confirm the success of the coating process. The synthesis of Mn NMOFs, their coating with a thin silica shell, and ensuing functionalization with acyclicarginine-glycine-aspartate (RGD) peptide and a fluorophore, and the application of such core-shell nanostructures in MR imaging has also been reported with the silica coat facilitating further functionalization with flourophore and a cell targeting peptide [108]. Rocca et al [106] in the same light equally achieved success in surface functionalization of Gd^{3+} based NMOFs with silica and found that the polymer coating slows the release of Gd^{3+} and also provide sites for the attachment of chemotherapeutics. Li and Zeng have [109] reported on a general method to enhance the relative hardness and toughness of MOF through deposition of mesoporous SiO_2 on the MOF using solution based processes. The SiO_2 was converted to mesoporous range to avoid challenge of pore blockage by the silica range and the ZIF-8 regrown in the internal space to give ZIF-8@mSiO_2 or ZIF-8@Au@mSiO_2.

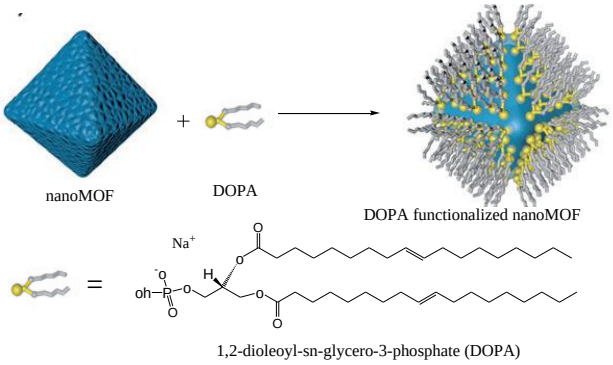

Figure 17: Surface Functionalization of NanoMOFs with DOPA [110]

This procedure permits the synthesis of complex structures such as growing another thin film on the mSiO_2 coating. Wang et al [110] have surface functionalized a series of three nanoMOFs UiO-66 ($Zr_6O_4(OH)_4$-$(BDC)_6$), UiO-67 ($Zr_6O_4(OH)_4(BPDC)_6$) and BUT-30 ($Zr_6O_4(OH)_4(EDDB)_6$) with 1,2-dioleoyl-sn-glycero-3-phosphate (DOPA). IR and NMR were used to confirm the success of the functionalization. The presence of DOPA on the surface of the MOFs was found to enhance the dispersibility of the MOFs in solvent in contrast to the unfunctionalized MOFs which readily aggregate in solvents. A similar has been reported by Jung and Park [107] who accomplished dual functionalization of a Zr based MOF. Pendant surface -NH_2 functions were used to conjugate fatty acids to the surface whereas *candida antarctica lipase*, CAL-B a well-known biocatalyst in organic synthesis was conjugated to the pendant carboxylate ends of the MOF linker. The CAL-B functionalized MOF unlike the unfunctionalized MOF showed hydrolysis activity. Zhao et al [111] and Lazaro et al [105] achieved surface modification by sequential azide and PEGylation to obtained water stable MOFs. As a result of the fact that in some cases MOFs will be used in environment containing both water and organic compounds, Sun et al [112] achieved improved amphiphobicity of ZIF-8 MOF by coating the external surface with perflouroalkyle groups. After controlled functionalization of the exterior amphiphilic surface with perfluoroalkyl groups via thiol-ene reaction, the ensuing MOFs exhibited both superhydrophobicity and oleophobicity, with the crystallinity and porosity intact. The use of a bulky species for coating restricted the coating to the outer surface and increased the stability of the MOF. The stability of the MOF upon exposure to 100% relative humidity under CO_2 atmosphere at 45 ^oC confirmed the enhancement ability of coating. Wuttke et al [76] developed novel metal–organic framework nanoparticles and

surface functionalized by encapsulating with a lipid membrane using the lipid DOPC (1,2-dioleoyl-snglycero-3-phosphocholine) in order to carry out drug delivery studies. They demonstrated that the MOF/lipid system can effectively store dye molecules inside the porous scaffold of the MOF while the lipid bilayer prevents their premature release. Moreover, for MIL-100(Fe) the lipid bilayer drastically increases the colloidal stability of the nanoparticles.

4.5 Post Synthetic Cluster Modification

Other than restricting PSM to the linkers or the surface of the MOF, the metal nodes or inorganic clusters can as well be exploited to offer additional functionalities to the MOF. Nodes/cluster functionalization arises from the fact that many MOFs contain coordinate unsaturated metal sites where non-bridging ligands can be added in a PSM workup; additionally, non-bridging exchange facilitated by acid or base chemistry of the leaving and entering ligands or some other external factor such as heat can be carried out at the nodes thereby altering the functionality of the MOF [113]. The attachment of ligands at the node/cluster could therefore be either through coordinate bonds (when there exist unsaturated coordinate sites) or ionic bonds (when the ligand exchange is facilitated by the acid-base chemistry of the exchanging ligands). Islamoglu et al [97] have reported on post synthetic modification of mesoporous Zr-based MOF NU-1000 using three protocols namely; solvent-assisted ligand incorporation (SALI), atomic layer deposition in MOFs (AIM) and solvent-assisted linker exchange (SALE), otherwise referred to as postsynthethic exchange, PSE already discussed. While SALI involves replacing labile ligand, nonstructural inorganic ligands with functional organic ligands, AIM is effective for installing single metal complexes or metal-containing clusters using nodes as supports. Whereas carboxylates could not be installed unto the metal nodes, their phosphate counterparts were successfully installed. The authors used the concept of atomic layer deposition to install metal oxide and sulfide films on the metal nodes of the MOF without compromising the crystal structure and porosity. The metal oxide functionalized MOFs showed good catalytic activity for gas phase hydrogenation of ethylene and alkene oligomerization while the metal sulfide functionalized MOF proved to be a good photocatalyst owing to the presence of the sulfur.

Beyond incorporating ligands through the replacement based on their acid-base properties, intentional creation of defects at binding sites in MOFs and subsequent incorporation of ligands is another approach that has recently emerged. Defective MOFs in themselves have attracted lot of interest owing to their impressive properties in catalysis and as well PSM [114]. Wu et al [115] exploited this concept to obtain intentional defective UiO-66 with missing linkers using varying concentrations of acetic acid modulator and reaction time. The authors found that tuning the linker vacancy using reaction time and modulator concentration brings about exceptional porosity in the resulting MOF. DeCoste et al [116] used a procedure developed by Katz et al [117] to obtain defective UiO-66 in which terephthalic linkers were missing; these vacancy sites were subsequently filled by incorporation of oxalic acid via solvent assisted ligand incorporation. The oxalate attaches only through one of the carboxylate leaving the other carboxylate free in the MOF. The oxalate functionalized MOF demonstrated improved capacity in octane and NO_2 compared to the unfunctionalized defective and defect free MOF. Deria et al [114] carried out water stabilization of Zr_6-based MOF via solvent-assisted ligand incorporation at the nodes.

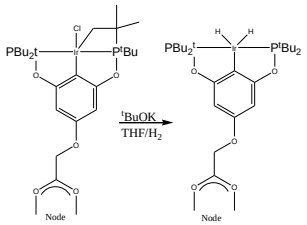

Figure 18: Activation of Ir complex [118].

The authors established that, the presence of non-bridging hydroxyl and aqua ligands of the Zr_6-nodes of the mesoporous MOF NU-1000 [molecular formula $Zr_6(\mu_3\text{–}O)_4(\mu_3\text{–}OH)_4(\text{–}OH)_4(\text{–}OH_2)_4(TBAPy)_2$; H_4TBAPy = 1,3,6,8-tetrakis(p-benzoic-acid)pyrene] can assist a variety of node-functionalization patterns such as metalation via AIM and grafting organic chemical functionalities via SALI. To this end, NU-1000 was functionalized by replacing polar hydroxyl and aqua ligands with aprotic, non-polar organic carboxylates at the Zr nodes. The incoming non-polar groups resulted in the reduction of pore volume and as well protected the Zr node so that its interaction with water molecules reduced and the stability of the MOF was enhanced. Rimoldi et al [118] have expanded on SALI to install a catalytically active iridium pincer complex in NU-1000 MOF. Suspending NU-1000 in a toluene solution of the iridium complex at room temperature 24 hrs, led to the installation of the complex at the Zr node of the MOF as indicated by color change from yellow to orange with the morphological integrity unchanged. The pincer complex was then obtained by reaction the MOF-Ir complex with tBuOK and H_2 in DMF to give the NU-1000 supported dihydride iridium pincer complex. Spectroscopic analysis revealed that the crystallinity and porosity of the framework are retained indicating the preservation of catalytically active sites of the Ir complex. Heterogeneous catalyst shows enhanced activity with respect to its homogeneous counterpart and reveals stability upon prolonged use. Dolgopolova et al [119] carried out stepwise building of hierarchical complexity in actinide metal–organic frameworks. A series of four MOFs (Th_6-Me_2BPDC-10; Me_2BPDC^{2-}=2,2′-dimethylbiphenyl-4,4″-dicarboxylate, U_6-Me_2BPDC-8, Zr_6-Me_2BPDC-8 and Th_6-TPDC-NH_2-12; TPDC-NH_2^{2-} =2′-amino-terphenyl-4,4″-dicarboxylate), were prepared using the solvothermal method and used as precursors for various post-synthetic workups. The presence of unsaturated sites on the nodes of Th_6-Me_2BPDC-10 and U_6-Me_2BPDC-8 facilitated the possibility of node extension and capping linker installation for which both processes were found to occur by single-crystal-to-single-crystal transformations. The choice of capping linkers is determined by the size of the pocket between metal nodes in a parent framework, where additional linkers can be installed. While the capping linker TPDC-NH_2 could be successfully installed, the authors equally showed that heating Th_6-Me_2BPDC-10 together with $ThCl_4$ and HTPDC-NH_2 leads to the simultaneous incorporation of Th^{4+} as guest into the MOF and HTPDC-NH_2 as capping linker. Further transformation of the capping linker using diethoxyphosphorylurea (DEPU) introduced groups for selective actinide binding rendering the MOF a good candidate for uranium extraction from seawater.

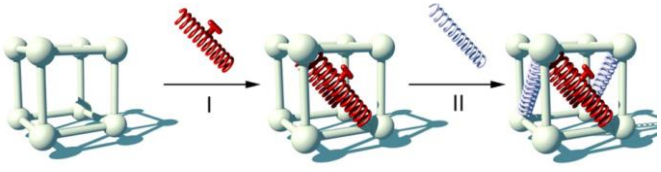

Figure 19: Sequential installation of capping linkers [119]. *© permission ACS 2018*

Sequential installation of H_2TPDC-DEPU (for UO^{2+} covalent anchor) and naphthalene-2,6-dicarboxylate NDC^{2-} was also demonstrated to be possible owing to the different sizes of the pockets. The extension or transmetallation of the MOF was accomplished by either heating or soaking the MOF in a desired species. Using $ThCl_4$ and U_6-Me_2BPDC-8 resulted 94 % exchange even though Zr_6-Me_2BPDC-8 could not be successfully transmetalated though it structure is similar to that of U_6-Me_2BPDC-8. Yuan et al [120] had earlier used the idea of sequential ligand installation to modify PCN-700, a Zr-MOF with eight-connected. $Zr_6O_4(OH)_{8(}H_2O)_4$ clusters with transformations taking place by means of single-crystal-to-single-crystal. The presence of two types of pockets, flexibility and stability of the Zr based MOF are requirements which qualify a MOF for such type of modification. By sequentially exposing the crystals to solutions of H_2BDC and H_2Me_2-TPDC in DMF at 75 °C for 24 h BDC and Me_2TPDC were installed respectively into the short and long pockets of the MOF. It was found that reversing the order and beginning with Me_2TPDC followed by H_2BDC did not lead to the installation of the BDC attributed to the fact that, Me_2TPDC occupied all the pockets making it impossible to install the BDC. The sequence of installation therefore proved to be crucial in this case.

4.6 Metalation

The incorporation of metal ions or clusters into an already synthesized MOF is another approach to carrying PSM. There are four general approaches to post synthetic metalation including addition of functional group bearing a metal ion attached at one end, exchange of counter ion in a charged MOF, growth or encapsulation of metal nanoparticles inside a framework, and cation metathesis at the metal nodes [121]. This review shall however only give a general view of metalation, detailed review of post synthetic metalation has been reported by Evans et al [121]. Generally, the presence of pendant functional groups such as -OH, -SH, -COOH and -SO_3H render metalation easy [122]. Studies have revealed that, MOFs in which the linkers contain pendant –SO_3H or –COOH functional groups can easily be post functionalized with alkali metal cations using the hydroxide solutions of the alkali metals [92]. Manna et al [123], [124] metalated UiO-66-CAT-M [M = Cr(iii), Fe^{3+} or Ga^{3+}] and UiO-66-TCAT [T = Pd or Ir] to obtain bpy-UiO metalated MOFs whose crystallinity is similar to bpy-UiO. XRD showed that the introduced metal ions are attached to the nitrogen atoms of the bipyridine rings. The Zr/Ir and Zr/Pd ratios were established using inductively coupled mass spectrometry. Similar reports by Zheng et al [125] have achieved successful metalation of a Cu based MOF with Tb^{3+} with unchanged structural integrity for H_2S detection. While the high thermal and water stable Cu1 MOF could easily be post functionalized with Tb^{3+} due to the presence of reaction sites, Cu2 counterpart could not. Snurr et al used *ab initio* and grand canonical Monte Carlo (GCMC) simulations to evaluate the effect of post synthetic metalation of metal organic frameworks on H_2 storage capacities of MOF at ambient temperature using various M-alkoxides for functionalization (M = Li, Be, Mg, Mn, Fe, Ni, Cu, and Zn) and studying their interaction with H_2 using MP2 and M06 quantum mechanical calculations [105-107].

Occasionally, MOFs contain functional groups unto which metal ions or species cannot be introduced; such functional groups therefore protect the introduction of metal species. This obstacle can be overcome by post synthetic deprotection (PSD) a process whereby the protected functional group is cleaved using external influence so as to reveal a desired functionality [92].

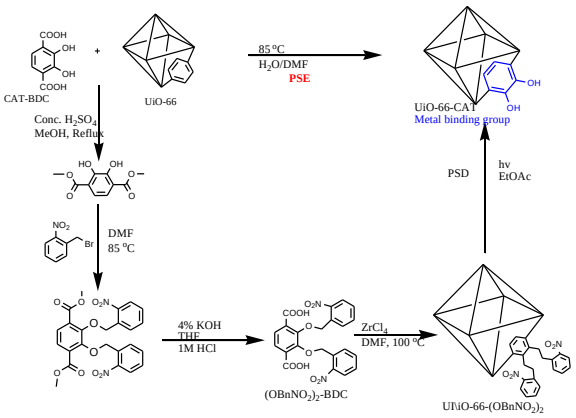

Figure 20: Synthetic Scheme for UiO-66-CAT via PSD and PSE.

To this end, Fei et al [127], isolated metal-monocatecholato moiety in a metal–organic framework (MOF) by two essentially different postsynthetic approaches namely; postsynthetic deprotection (PSD) and postsynthetic exchange (PSE), Fig. **20**. While the PSD proceeds via a series of steps, PSE proceeds via a single step and is therefore desired for the facile nature. Subsequent incubation of the UiO-66-CAT crystals in separate solutions of $Fe(ClO_4)_3$ and K_2CrO_4 resulted in the metalation of the UiO-66-CAT MOF with Fe and Cr binding to the OH group of the catechol. X-ray analyses of the metalated samples reveal little compromise in the structural integrity of the functionalized MOFs. UiO-66-Cr-CAT proved to be an efficient and "green" alcohol oxidation catalyst for a range of substrates. In addition to the above discussed post synthetic strategies, there have emerged other post synthetic strategies. Li et al [128] developed a method in which a MOF bearing two types of functional pores was selectively functionalized in a stepwise fashion. The MIL-101-Cr $\{Cr_3(F)(H_2O)_2O[(CO_2)\text{-}C_6H_4(CO_2)]_3\}$ possess a large and small cage connected by a small window. Selective multiple functional strategies can achieve MOFs with varied applications. The internal surfaces of the cages were first functionalized by addition of ethylenediamine and subsequent addition phospotungstic acid leads only to the functionalization of the large care due to the large size of the acid compared to the small pore of the small cage. The third step involved grafting of terepthalic ring to the amino group of the small cage. This strategy conferred the MOF with amphoteric property arising from the phospotungstic acid and diamine.

4.7 Guest Inclusion as a strategy for PSM

Another aspect which has also gained considerable traction especially with flexible MOFs with regards to PSM is guest inclusion. The inclusion of guest into a MOF maybe is an attractive approach to rationally tune or modify both physical properties such as magnetism, luminescence as well as tune framework flexibility and response to such changes as temperature and pressure [129]. The interaction between host and guest could either be electrostatic such as the case solvent guest or by means of chemical bonds such as the case of most metal nanoparticles guest. Zhang et al have further indicated that the interaction between host and guest can be so strong to the extent that there is a resultant thermal expansion of the MOF leading to what has been referred to as thermal expansion of flexible MOFs. Proof of this concept has been demonstrated by Zhang et al, who obtained an ultramicroporous MOF demonstrating an abrupt thermal expansion upon inclusion of DMF as guest as heating approaches the melting point of the guest due to conformational changes of the DMF. Parallel studies have also been reported by Kim et al [130] and Phillips et al [131]

using $Zn_2(BDC)_2(DABCO)$ [with DMF and benzene guest] and single-network $Cd(CN)_2$ [with CCl_4 and N_2 guest] respectively. The introduction of noble metal nanoparticles and /or other desired species as guest into MOFs for various applications ranging from photocatalysis, catalytic hydrogenation, and charge transfer amongst others has equally been reported [132–136]. While introduction of metal NPs can be done post synthesis, Xiao et al [134,136]and Zhang et al [137] have equally noted the possibility of achieving the introduction of Pt NPs into UiO-66-NH_2 in situ. This approach is commonly used when the guest possesses certain desirable properties. Chowdhuri et al introduced Fe_3O_4 into porous isorecticular metal organic frameworks (IRMOF-3) by simply mixing the MOF and Fe_3O_4 in appropriate solvent and ratio and maintaining at 100 ^{o}C in autoclave for 4 hours. Gao et al on their part imparted fluorescent property unto Fe-MIL-53-NH_2 by guest inclusion of 5-carboxyfluorescein (5-FAM). Similar work by Yang et al [138] successfully achieved the regulation of spatial distribution of nanoparticles within MOFs for improved catalytic efficiency with the nanoparticles confined closer to the surface of the MOF. The restriction of the metal nanoparticles to the surface could be regulated by tuning the crystallization behavior of the MOF at different concentration. At low ligand concentration, the metal nanoparticles were found to be located mainly at the outer surface whereas at higher concentration the inner surface of the MOF.

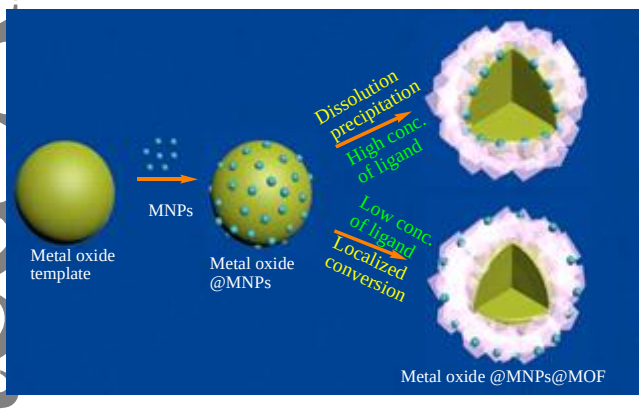

Figure 21: Spatial localization regulation of MNPs within MOF crystals via template-sacrifice method [138]

Parallel reports by Zhang et [137] have indicated the successful installation of Pt nanoenzyme on photosensitizer integrated MOFs for photodynamic therapy via in situ reduction.

5. Biological Applications of MOFs

The scope of applications of MOFs has since initial reports stretched beyond the traditional applications in catalysis, gas storage and separation into the area of biomedical because of the interesting characteristics of these MOFs ranging from porosity to the dual organic inorganic nature. As already stated, biomedical applications of MOFs range from the use as delivery vehicles for biologically active ingredients, BioMOFs, imaging theranostic and most recently sensing of biological molecules [19]. Important factors that warrant consideration along this line of application of MOFs include biocompatibility, toxicity as well as hydrothermal stability. Certain features make MOFs good candidates for biological applications including:

- Large specific surface area and pore volume which is associated with high sorption capacities of different guest molecules
- Ease of functionalizable cavities, where specific host–guest interactions may take place, allowing the regulation of the sorption processes
- Adequate stability profile under physiological conditions, remaining stable enough to carry out their function and, being removed later from the body, preventing related potential toxic effects due to endogenous accumulation and
- Possibility of synthesizing nanoscale crystals which has an important influence on in vivo fate and applications [139]

The section that follows will examine some biological related applications of MOFs.

5.1 Delivery systems

Drug delivery systems DDSs have emerged as an important area of research as a consequence of the fact that conventional modes of administration usually involve large doses which often lead to systemic circulation with the drugs reaching and exerting effects at unintended targets [140]. In addition, a DDS is also necessary in the case where a drug molecule is not soluble in body fluid [141]. A drug delivery system will ideally transport an active compound to a specific site, release the active compound and is either eliminated or undergoes degradation. To qualify as an efficient DDS, the delivery vehicle must meet certain requirements including:

(a) Control release of the active compound and avoid "burst effect" (a situation whereby the drug is release from the DDS prematurely). In this respect, it has been hypothesized that release of drugs from MOFs can occur through the desorption of adsorbed drug from the surface of the sphere, diffusion of drug through the sphere and release through the erosion of the sphere [140].
(b) Control matrix degradation and possibility to engineer the surface of the delivery vehicle
(c) Be detectable by various imaging techniques
(d) Possess high drug loading capacity and do so with efficiency.
(e) Toxicity and biocompatibility [15, 113-114],

Until recently, the most widely researched DDSs included either inorganic materials like mesoporous silica, silicon or organic materials like micelles, liposomes, functional hydrogels, nanoparticles amongst others. Whereas organic materials are characterized by relatively good biocompatibility, appreciable loading capacities and lack of good control delivery profile, inorganic materials on the other hand are characterized by poor loading capacity, poor compatibility and better release control profiles [19]. It is in this light that MOFs take advantage of their organic and inorganic components drawing the advantages of both that they present as good candidates for DDSs. One of the main benefits of using MOFs as DDS lies in their favorable structural architecture and diversity [143]. MOF carriers at nanoscale can allow for better control of drug plasma levels, thereby increasing the efficiency and decreasing the toxicity [144], [142]. They can also lead to an increase in the drug stability by means of protecting the drug from biodegradation. The possibility to tune the pore and pore structure (by means of judicious choice of precursors), carry out post synthetic modifications [46] and include targeting ligands such as peptides or nucleotides in MOFs that can trigger drug release to diseased tissues (*e.g.* tumor regions) [145] are factors which collectively render MOFs more credible candidates for the purpose of DDSs. Another aspect that make MOFs more attractive as DDSs is the fact that a single MOF can be used to deliver multiple active compounds since some of these materials display a dual hydrophilic/hydrophobic pore structure [146]. This new discovery of delivering multiple therapeutic agents with MOFs is particularly attractive because it broadens the spectrum of combination therapy; an approach wherein a single disease is

treated with multiple drugs especially when the different therapeutic agents work together in some fashion or when issues such as drug resistance arise and warrant prevention or limitation [143]. Proof of this concept has been reported by McKinlay et al [143] who demonstrated the simultaneous delivery of NO and antibiotic metronidazole in phosphate buffered saline PBS. The porous and good binding of large quantities of NO to both HKUST-1 and the M-CPO-27 (M = Ni and Co) and subsequent release upon exposure to moisture was exploited to successively load and deliver NO and metronidazole. The fast release first step of NO leads to the sudden dead of majority of the bacteria while allowing the microbial burden on the materials to be kept low through the slower second stage delivery of larger anti-bacterial guest molecules such as the antibiotic metronidazole. The final step involved the release of metal ions form the MOF which also showed antibiotic activity. The authors interestingly found that the presence of metronidazole within the pores of the MOFs slows the release of NO as much moisture is required to trigger the release. These results suggest that the presence of more than a single guest in the pore of of a MOF could enhance the release profile. Rojas et al [146] studied the simultaneous delivery of [Ru(p-cymene)Cl_2(pta)] (pta = 1,3,5-triaza-7-phosphaadamantane) RAPTA-C and the biologically active gas NO using a nickel based MOF CPO-27-Ni as a delivery vehicle. The moisture triggered release of chemisorbed NO appears to occur much slower taking up to 12 hours possibly as a result of the presence of RAPTA in the voids. The rapid release of NO may have a beneficial effect in biological applications due to the vasodilation properties of this signaling molecule, which could facilitate the penetration of RAPTA-C into the cancer cells. Zhang et al [144] have also showed proof of this concept using rationally designed pH responsive MOF nanocarriers ZIF-8 for the co-delivery of doxorubicin hydrochloride DOX,/verapamil hydrochloride VER, for multidrug resistance MDR cancer therapy. The polyethylene glycol folate PEG-FA showed high drug loadings (8.9% and 32% for DOX and VER respectively), good stability, biocompartibility as well as high cytotoxic activity toward B16F10 and multidrug resistant MCF-7 (MCF-7/A) cells. With intravenous injection leading to accumulation of drug in cancer cells, the authors showed that at lower pH (pH =5, the pH for endosome in tumor cell) the amount of drug released is higher [(27.37 ± 0.92)% of DOX and (76.48 ± 0.68)% of VER] compared to [(9.68 ± 1.25)% of DOX and (18.18 ± 0.74)% of VER] higher physiological pH of 7.4 during a 24h period. These findings are salient since they indicate that successful applications of MOFs in delivery of cancer therapy could lead to reduction in systemic toxicity that is common with conventional administration routes. He et al [147] used nano MOFs to achieve simultaneous delivery of cisplatin to the cell nuclei and gene silencing siRNA. Whereas no cytotoxicity (cell viability of 96.2 ± 3.4%) was observed in SKOV-3 cells when treated with siRNA/UiO at 12 times higher siRNA dose, simultaneously delivering pooled siRNAs and cisplatin utilizing UiO nano MOFs led to the IC_{50} value dramatically decreasing by more than 11-fold compared to free cisplatin and UiO-Cis. While the practical applications of this approach may still be a while away, the results from these authors proof that DDS with MOFs could usher a millstone revolution in this field especially co-delivery of other nucleic acid drugs such as microRNA, and plasmid DNA. Illes et al [148] have recently used a liposome coated Lip-MIL-88A MOF to investigate the simultaneous delivery of anticancer agents irinotecan and floxuridine. Loading percentages of 21 wt% and 3.1 wt% for irinotecan and floxuridine respectively reported. Release profiles indicated that, liposome-coated MOF nanoparticles can serve as a DDS for dual therapy preventing burst effect and taking advantage of the delivery of two different drugs. Simultaneous delivery of two drugs however showed less efficiency compared to the delivery of single drug owing to the lower efficiency of floxuridine. These findings seem to contrast those of McKinlay et al thereby suggesting that the improvement of release profile with more than a single guest in MOF pore maybe case specific and not a general rule. Yang et al [142] have drawn from the fact that physiological pH of inflamed tissues post-surgery is in the neighborhood 5.4 to synthesize pH responsive DDS MOF for post-surgery therapy. Cationic nanocarrier MOF ZJU-101, with a large loading capacity toward anionic drug diclofenac sodium DS, was constructed by combining zirconium with 2,2′-bipyridine-5,5′-dicarboxylate (BPYDC).

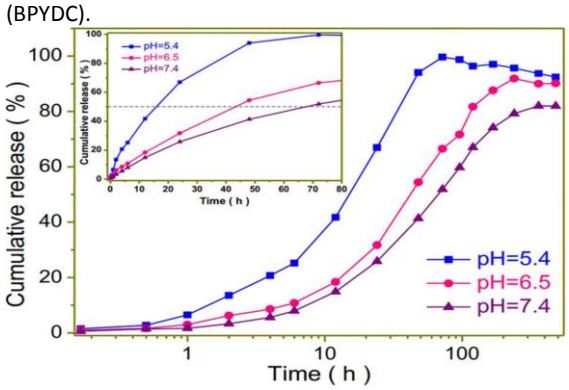

Figure 22: Release profiles of DS loaded ZJU-101 in the PBS of different pH values [111].

While the neutral MOF could not load any drug even after stirring the drug/MOF mixture for up to seven days, stirring in trifluoromethane for 24 hrs leads to the conversion of 56.6 % of the N atoms in BYPDC to N^+-CH_3 creating charge which facilitate ionic interaction between the drug and MOF and loading rate up to 0.546 g/g, which is the highest loading capacity in comparison with those of other typical ionic MOFs used in biomedicine. Whereas there occurs rapid release of an estimated half of the loaded drug for around 15, 42, and 65 h at PBS of pH = 5.4, 6.5, and 7.4, respectively in PBS (pH of inflamed tissues), the DDs showed no 'burst release', typical expectations of an ideal DDS. The rapid release was explained by the fact that there exist higher ion concentration at lower pH which leads to ion exchange between anions in PBS of pH = 5.4 and coordinated/free diclofenac in MOF occurs more often, discharging the Coulombic interactions between the positive charge of the MOF material and negative charged drug.

Table 1: Drug Loading Capacity of Different anionic/cationic MOFs and the BET Surface/Pore Size

MOFs	Framework character	BET surface or pore size	Drug loading Capacity g/g
ZJU-101 [142]	Cationic	561 m^2/g	0.55
MOF-74-Fe(III) [149]	Cationic	11 Å	0.19
Bio-MOF-1 [150]	Anionic	1700 m^2/g	0.22
Zn-TATAT [151]	Anionic	20 Å	0.5
$(NH_2(CH_3)_2[Zn_3(L^*)_2\cdot 3.5DMF]$) [152]	Cationic	14.2 × 14.5 $Å^2$	0.225

L* = 1,1′,4′,1″,4″,1‴-quaterphenyl-3,5,3‴,5‴-tetracarboxylic acid 1,3,5-benzenetrisbenzoate

Luo et al [153] in the same light have similarly found that the release of cancer drug 5-fluorouracil 5-FU, from a low toxicity Zn based MOF is higher (98 %) and more controlled at lower pH (pH = 6) than at normal physiological pH = 7.4 in PBS solutions where only 62 % of the drug is released after 72 h. Parallel studies with 5-FU and a Cu based polyhedral metal–organic frameworks

(PMOFs) have shown akin release profile pattern and toxicity [154]. Additional sites for interaction between the MOF and drug can be created by heating the as-synthesized MOF to generate coordinative unsaturated copper sites on the Cu atoms in the MOF. Ahmad et al [155] used an unconventional method to obtain a series of porous coordination materials consisting of Cu-MOP, ligand and metal ions *via* click reaction and further coordination with metal(II) ions. The CuMOP-ligand-metal could be engineered to contain two different types of metal atoms; Cu:Cu; Cu:Zn; Cu:Co; Cu:Ni etc linking them with *4*-azidobenzoate (N_1) or 5-azidoisophthalate (N_2) to generate CuMOP-L-M(II) with approximately twelve coordinated sites around each MOP and thereby creating interconnected supramolecular pores which favor multifold encapsulation and release of drug molecules. These MOFs showed higher drug loading (40%) compared to their traditional counterpart Cu-L MOF (19.49 to 23.76%) for caffeine and 5-FU. Release profile in PBS at pH = 7 at 37 ^{o}C indicated a steady and controlled release lasting up to seven days. Beyond relying on physiological pH to achieve controlled delivery, Orellana-Tavra et al [156], [76] used chemical amorphotization to control delivery of fluorescent model molecule calcein and anticancer drug a-cyano-4-hydroxycinnamic acid (α-CHC) from a family of Zr-based metal–organic frameworks (MOFs) with different functionalized (bromo, nitro and amino) and extended linkers. The calcein showed poor loading (15.2%) owing to its large size compare to the α-CHC whose loading was twice as much. Confocal microscopy revealed that all the materials were able to penetrate into cells, and the therapeutic consequence of a-CHC on HeLa cells was boosted when loaded (20 wt %) into the MOF with the longest linker. Calcein release from the crystalline MOF occurred within two to three days giving a burst effect during the first hours of release, whereas the profiles from the amorphous counterparts were different in each case lasting up to 15 days. α-CHC release however showed no variation between crystalline and amorphous material. Tian et al [157] achieved both chemo- and photothermal therapy by using zeolitic imidazolate framework-8 (ZIF-8) as drug nanocarriers and implanted graphene quantum dots (GQDs) as local photothermal seeds. Their one-pot-synthetic approach yielded an approximate loading efficiency of 90% of doxorubicin (DOX) in the ZIF-8/GQD, with the DOX loading capacity in the ZIF-8/GQD nanoparticles estimated to be 47 μg/mg. The release profile indicated that at lower the pH, higher amount of drug is released conforming with other reports [149]. The framework showed irregular morphology at lower pH and longer immersion time as a result of decomposition which prompts further release of DOX. Irradiation of the GQD with near infrared (NIR) generates heat which destroys cancer cells by approximately 84%. The pH dependent property of the system implies its application can limit release of the drug molecules and GQD at unwanted destinations. Erucar and Keskin [158] beyond drug delivery with biocompatible MOFs investigated delivery of cosmetic molecules caffeine and urea. Initial agreements of storage between simulated and experimental values motivated the authors to extend their investigation to a series of 24 biocompatible MOFs for which they found these materials serve as good candidates for storage of ibuprofen, caffeine and urea as they outpaced traditional zeolitic and mesoporous silica drug storage materials. Cunha et al [159] had earlier reported on the encapsulation and delivery of caffeine using a series of MIL and UiO. The encapsulation of caffeine has presented a challenge in the cosmetic industry due to its high tendency to crystalize leading to poor loading and consequently release and low efficiency. However, by simple impregnation and suspension of the dehydrated MOFs in water or ethanol caffeine solutions for 72 hrs, the authors reported payloads reaching 50 wt %. Release profiles surveyed in simulated serum fluid (phosphate buffer solution (PBS) 0.04 M at pH = 7.4) or pure water (pH = 6.3) indicated that except for the MIL-127 and MIL-53 materials, most of the caffeine (53%, 68%, 79%, 93%, and 100% for MIL-53-Br, UiO-66-NH_2, MIL-100, UiO-66, and UiO-66-Br, respectively was release through 'burst effect' which in some cases was attributed to amorphotization of the solids or degradation of the MOFs. Li et al [140] have reported on the encapsulation of 5-Flourouracil (5-FU) in KHUST nanoMOFs by suspending the vacuum dried MOFs in ethanolic solution for several days at room temperature in the ratio 7:1 5-FU:MOF respectively for four days reaching loading percentage of 40.22 %. Release profiles indicate that, approximately 90% of the non-encapsulated drug was found in the release medium, while only 60% of the drug was released from NPs after approximately 10 h despite relative "burst effect" ascribed to diffusion of the surface adsorbed drug into the release medium. The release profiles indicated two phases with the first short-lived (typically zero order because of concentration independence) producing the desired pharmacological effect while the second phase was prolonged (resulting from the gradual erosion of the carrier) and performed a rather maintenance role during the course of administration. The release profiles can be modeled by the equation.

$$q_E - q_t = q_E^{-kt} \qquad [160]$$

Where q_E and q_t are the amounts of RAPTA-C released per gram of MOF (mmol g^{-1}) at equilibrium and at the time t (h), respectively, and k is the first order kinetic constant (h^{-1}). The authors speculated that a DDS MOF could be made to reach its target by reducing the amount of drug adsorbed on the surface. The question of speed to reach the target and amount of drug loaded is therefore another aspect that may warrant further investigation as there will be need to deliver a drug molecule in time enough and in good enough amount before a disease continues to spread. In vitro cytotoxicity studies revealed that at low concentrations the carrier is relatively safe avoiding safety concerns which have also been at the center of MOF research for biomedical applications. Haydar et al [141] have equally observed a similar two phase release profile using a series of MIL MOFs (53, 100 and 101) and Ca-MOF to deliver flurbiprofen (FBP), a nonsteroidal anti-inflammatory agent, which is known to be practically insoluble in aqueous solution. The success of the experiment illustrates a case where DDS can be used to overcome solubility related issues. In a related study, Rojas et al [160] used MIL-100(Fe) to deliver metallodrug [Ru(p-cymene)Cl2(pta)] (RAPTA-C) in simulated body fluid supplemented with bovine serum albumin (SBF@BSA, 5.4% w/v) which is known to slowdown the degradation rate of the MIL-100(Fe) nanoparticles and improve their colloidal stability. The delay and subsequent release of 80% of the loaded drug after three days in SBF@BSA has been ascribed to the presence of the albumin which probably reduces the rate of leaching of the MOF as indicated by the low concentration of 1,3,5-benzenetricarboxylate in solution compared to the case where only SBF was used while speeding up the rate of diffusion of the drug from the MOF pore into the SBF. Zhou et al [78] have reported on the selenium-containing polymer in ZIF-8 MOF nanocomposites as an efficient multi-responsive drug delivery system. The authors postulated that by functionalizing the MOF to obtain PEG-PuSeSe-PEG, it could act as a gatekeeper to delay drug release due to pH responsiveness and the fact that the drug must diffuse through the shell before release. The nano MOFs were grown on doxorubicin loaded micelles (DOX@P) template reaching efficiency of 19.1%. Release profiles indicate that once internalized in cells, release from MOF is easily triggered by low pH and presence of hydrogen peroxide. Alsaiari et al [161] have used ZIF-8 to deliver combined protein clustered regularly interspaced short palindromic repeat (CRISPR) associated proteins 9 (Cas9) with gene editing potential and single guide

RNA (sgRNA) which is used for site recognition when carrying out gene editing. CRISPR/Cas9 technology has been reportedly used as a therapeutic strategy against virus bacteria and cancer [133,162,163]. The coencapsulation of Cas9 and sgRNA attained 17% and the release was evaluated at different pH values viz: 5, 6 and 7.4. While only 3% release was observed at physiological pH of 7, 60% and 70% were respectively released at pH 6 and 5 during ten minutes.

5.2 Imaging

One of the recurrent challenges in drug delivery is how to track the delivery vehicle and as well evaluate the therapeutic effect. In this context, the applications of MOFs in biological systems should go beyond just loading an active agent and delivering, but as well provide a possibility of tracking the MOFs once released into the body. The advent of molecular imaging has paved way for noninvasive assessment of pharmacokinetics and curative processes with the use of contrast agents. Imaging approaches could either make use of luminescence or magnetic properties, with the later more frequently reported in literature especially in applications involving MOFs probably due to the fact that it makes use of non-ionizing non-radioactive radiation to produce images. The importance of contrast agents as diagnostic tools cannot be overemphasized, at present MRI require administration of high doses of contrast agents to overcome persistent low sensitivity of the technique. The use of MOFs could lead to a reduction in the dose amount capitalizing on the quantity of metal clusters located within the structure [164,165]. Judicious choice of starting materials (such as using magnetic and superparamagnetic moieties) and objective engineering together with PSM are important factors worth considering for this purpose. Privileged by their tunable sizes and surface properties, MOFs offer the opportunity of performing imaging and therapy simultaneously by either loading a contrast agent together with a drug molecule or inclusion of a contrast agent such as Gd^{3+} within the structure of the MOF [9]. The concept of imaging has been widely researched with nano oxide particles such as those of iron where the magnetic properties of iron are made use of.

Luminescence or optical imaging on the other hand operates on the principle that, visible light can be used to excite dye molecules within a tissue; the relaxation thereof used to either tract the position of the dye and/or destroys diseased tissue. This technique is frequently used for in vitro and ex vivo studies but is however limited by poor tissue penetration when it comes to in vivo applications [106].

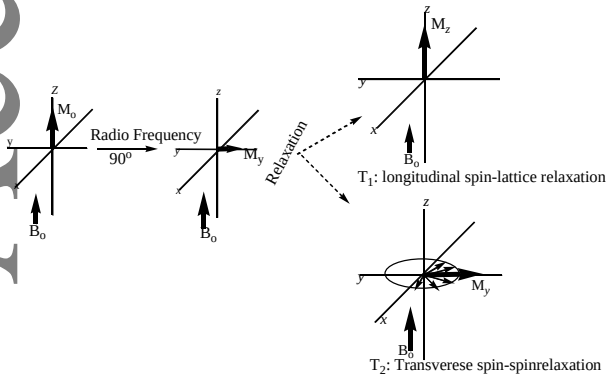

Figure 23: Excitation and relaxation modes of proton exposed to pulsating radiofrequency

MRI on the other-hand works on the principle that when a pulsating radiofrequency is applied to a proton inside a magnetic field B_o, the proton excites longitudinally and would relax either longitudinally or transversely. Given the fact that MRI has low sensitivity, relaxation times can be shortened by use of contrast agents CAs. The ability of the CAs to do so is known as relaxivity for which there are two types; longitudinal relaxivity r_1 and transverse relaxivity r_2. The ratio of r_1 to r_2 is used to classify CAs;

If $\frac{r_2}{r_1} \approx 1$,

We have a T_1 or positive contrast agent which leads to the production high signal-to-noise ratio and hence bright images. If the r_2**:** r_1 is far from 1, we have a T_2 (negative) CA which leads to reduction of signal to noise ratio and hence dark images. Knowledge guided choices should therefore be able to produce MOFs that not possess high drug payload but as well meet desired imaging properties. While a single imaging approach can be conveniently used, Gao et al [166] noted for the first time the possibility of magnetic resonance/optical dual mode imaging in which the MOF material is designed to contain both luminescent and magnetic materials. A MOFs/MOFs heterostructure was obtained by growing a luminescent lanthanide MOF in a magnetic iron MOF to obtain a structure possessing both luminescent and magnetic properties. Successful loading and delivery of 5-FU, and dual imaging prompted by the heterostructure was achieved with the MOF displaying high dispersibility and stability in simulated body fluid. Earlier on, Gao et al [166] investigated the synthesis of a smart MOF for MRI/ optical imaging and targeted drug delivery with a DDS Fe-MIL-53-NH_2-FA-5-FAM/5-FU [FA = folic acid, FAM = 5-carboxylfluorescein]. The MOF Fe-MIL-53-NH_2, served the dual task of loading the drug and MRI, FA used as targeting agent to study the efficiency of the delivering drug into tumor cells, and FAM was used as optical imaging agent. MRI analysis revealed a linear increase in $\frac{1}{T2}$ within the tested range suggesting the efficacy of the Fe MOF as a good MRI contrast agent. Luminescence imaging analysis revealed FA is a good targeting reagent whereas FAM is a good fluorescent agent. Drug release studies showed better sustained release of the 5-FU at pH of 5 compared to pH of 7. These results were consistent with report by Chowdhuri et al [133] who equally confirmed the efficiency of FA as targeting agent in Fe_3O_4@IRMOF-3/FA magnetic NMOFs as an MRI contrast agent. Images of cells incubated with Fe_3O_4@IRMOF-3/FA NMOFs exhibited better negative contrast improvement compared to the Fe_3O_4@IRMOF-3 NMOFs.

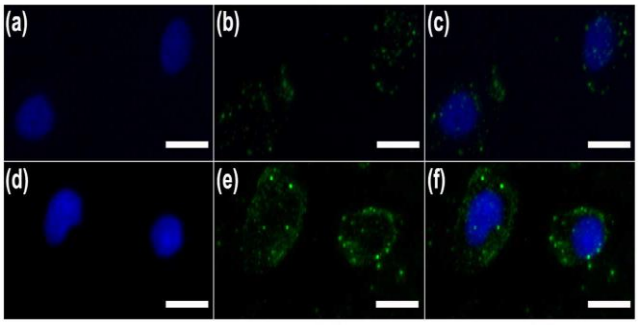

Figure 24: Luminescent Imaging. Inverted florescence microscope images of 293 cells (a–c) and MCF-7 cells (d–f) incubated with UCNPs@MOFDOX-AS1411 [167].

Rieter et al [30] investigated the potential of $Gd(BDC)_{1.5}(H_2O)_2$ and $[Gd(1,2,4\text{-}BTC)(H_2O)_3]\bullet H_2O$ nanorods and as potential multimodal contrast enhancing agents and observed unprecedented $r_1$values (of 35.8 s^{-1} per mM of Gd^{3+} and ~1.6×107 s^{-1} per mM of nanorod) for $Gd(BDC)_{1.5}(H_2O)_2$ with at least an order of magnitude higher than those of Gd^{3+}-containing liposomes which have been shown to be effective target-specific MR contrast agents for cancer and cardiovascular disease suggesting that this material stands a good chance of enhancing imaging. Deng et al [167] obtained aptamer-mediated up-conversion using β-$NaYF_4$:Yb^{3+}/Er^{3+} core and MIL-100(Fe) MOF

shell nanocomposites for targeted drug delivery and cell imaging with the fluorescent lanthanides covalently attached to the MOF at room temperature. Confocal laser scanning microscopy revealed that incubation with tissue prompts fluorescence of cancerous cells due to receptor mediated endocytosis of the nanocomposite containing the fluorescent material. The authors showed that the aptamer-functionalized upconversion luminescent nanomaterials as signal reporting groups could be potentially used as a diagnostic tool for the detection of cancer in early stage. Wang et al [168] reported on the multifunctional mixed-metal (gadolinium/ytterbium) nanoscale coordination polymers of bipyridine ligand for triple-modality imaging guided photodynamic therapy. Coating with PEG resulted to improve stability, increased blood circulation time, and enhanced biocompartibility. A 15.7 fold signal enhancement in fluorescence imaging, 33% and 64% MR and computed tomography imaging were observed after 30 minutes following intravenous injection in mice respectively leading to easy distinction of tumor cells from non-tumor cells. High efficiency of Photodynamic therapy PDT, was confirmed by the death of about 80% of diseased cells after injection of diseased tissue with the nanoscale polymer and irradiation with light emitting diode (LED).

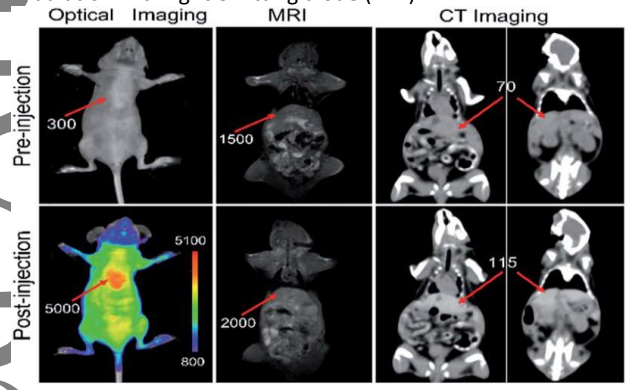

Figure 25: In vivo fluorescence, MRI and computed tomography images of mice injected with Gd/Yb complex PEGlated nanopolymers [168].

Taylor-Parshow et al [46] introduced 1,3,5,7-tetramethyl-4,4-difluoro-8-bromomethyl-4-bora 3a,4a-diaza-s-indacene (Br-BODIPY) as optical imaging contrast agent into MIL-101 MOF. The silica functionalized MOF was loaded with BODIPY and cancer drug ethoxysuccinato-cisplatin (ESCP). In vitro evaluation of the MOF-drug-contrast agent composite on HT-29 human colon adenocarcinoma cells using LSCM revealed fluorescent labeling in a dose dependent manner attributed to the slow release of BODIPY from the MOF after internalization. Horcajada et al [169] investigated the potential of a series of non-toxic iron(iii) carboxylate MOFs (MIL-53, MIL-88A, MIL-88Bt, MIL-89, MIL-100 and MIL-101_NH_2; nanoMOFs as contrast agents and found that three months after administration of rats with the MOF, the liver and spleen of the treated rats returned to same color as that of normal rats. Relaxivity value r2 of MIL-88A were of the order 50 s^{-1} mM^{-1} which is sufficient for *in vivo* application and increases slightly with PEGylation. This increase has been attributed to increase in the size of nanoparticles which possibly decreases aggregation. The presence of both coordinated and uncoordinated water molecules in the framework and interchange thereof prompts relaxation times of water protons and consequently good imaging properties

Another imaging technique uses near infrared radiation with luminescent materials emitting in this region considered important in biological applications for the following reasons:

- Biological material usually have low autofluorescence in the NIR window, making it easy to distinguish anticipated signal from background implying high signal to noise ratio and better sensitivity
- NIR light scatters less than visible light, so that there is increased optical imaging resolution
- NIR photons interact less with biological material compared with visible photons, thereby reducing the threat of disturbing or damaging the biological systems being observed [170–172].

Many lanthanide cations are known to emit in the NIR window with a narrower band (compared to that of many organic molecules) with their emission wavelength unaffected by environmental factors such as pH, biological environment, and resistance to photobleaching an aspect which enables them to be used repeatedly over a long period [172]. To this end Foucault-Collet et al [172] reported on lanthanide NIR imaging in living cells with Yb^{3+} nano metal organic frameworks. Incubation of the MOFs with HeLa and NIH 3T3 cells for 24 h and subsequent evaluation revealed Yb^{3+} emission signals with good sensitivity consequent of the high signal-to-noise ratio.

5.3 Luminescence and Non-Luminescent Based Biosensing applications

A biosensor is a devise with biological sensing component fitted or integrated within a transducer [165]. Chemical sensors must demonstrate desired selectivity, sensitivity, response times, material stability, and reusability. Owing to their porous nature, MOFs can possibly pre-concentrate the analytes within the pores and channels and in so doing providing an ideal environment to accommodate the analyte molecules thereby inducing specific recognition and thus enhancing sensitivity [173]. The versatile nature of MOFs as well means that they can be tailored to meet sensing demands either by means of loading the sensor into the pores, or by incorporating the sensor into the MOF structure or by means of PSM. Careful choice of building units can lead to MOFs with light absorption and emission properties that escape interference of the desired analyte. Sensing approaches could either be luminescent or non-luminescent depending on the properties of the MOFs.

The sensing properties of MOFs results from:

1. Channel size exclusion; wherein only the molecule with a specific size is allowed to access the pores
2. Specific coordination or hydrogen bonding of analytes to the framework
3. Analyte-specific signal response. Some analytes will quench luminescence while other others may significantly increase or decrease it. This interaction may therefore be used to identify the analyte.
4. Host-guest chemistry in the MOF cavity
5. The chirality of the framework before and after interaction with the analyte can be used to as well identify the analyte [173].

Miller et al [165] have noted that luminescence can either be quantitative or qualitative where the former involves selective interaction of the an analyte with a MOF and use of the luminescence property to visually observe the sensing and direct measurement in solution *in vivo* while the latter involves the use of a MOF's luminescence to locate and a visualize a cellular region of interest using optical microscopy. Our focus here shall however not be the details of quantitative and qualitative sensing but rather highlighting some papers that have proven the concept. The reader may consult Miller et al [165] for details on qualitative and quantitative aspects of luminescence sensing. As proof of concept, Rieter et al [174] attached silylated Tb-EDTA monoamide derivative to Eu-doped $Gd(BDC)_{1.5}$-$(H_2O)_2$@SiO_2 nanoparticles and used the Tb complexes and ions as molecular probe for anthrax and other bacteria. Addition dipicolinic acid DPA a major constituent of many pathogenic spore-forming

bacteria to the medium containing the functionalized NMOFs led to the clear luminescence resulting from Tb-EDTM-DPA complexation with intensity of the signal was found to increase with increasing concentration of the DPA and levels when the Tb-EDTA complexes became coordinatively saturated with DPA. The Tb-EDTM could therefore be used to probe the presence of DPA.

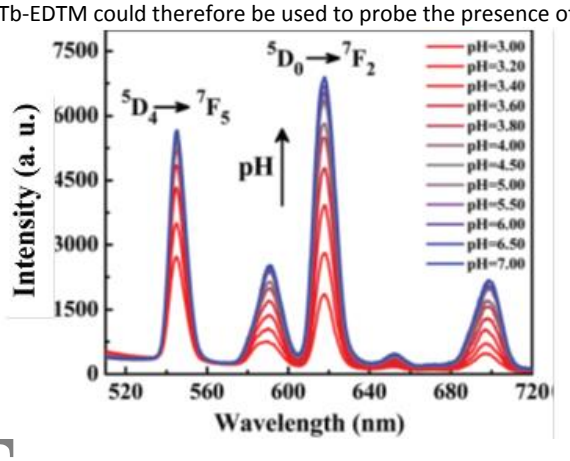

Figure 26: The variation of intensity with pH [175]

Xja et al [175] demonstrated the possibility of using a MOF to probe pH by synthesizing a mixed lanthanide NMOF and studying the luminescence of the MOF at different pH values. The $Eu_{0.034}Tb_{0.966}$-NMOF demonstrated characteristic lanthanide luminescence with sharp and well-separated emission bands with characteristic peaks representing the transitions $^5D_4 \rightarrow {}^7F_J$ of Tb^{3+} ions and the $^5D_0 \rightarrow {}^7F_J$ (J = 1, 2, 3, and 4) transitions of Eu^{3+} ions when excited at 340 nm. The authors found that, in acidic conditions, the luminescence intensity of Tb^{3+} and Eu^{3+} decreases gradually as the pH decreases whereas in basic conditions, the luminescence intensity of both ions decreases with a higher degree of aqueous alkali, and the decreasing rate of Eu^{3+} is slightly faster than Tb^{3+}. With these observations, they postulated that since abnormal conditions in the body such as the case of cancers are characterized by abnormal pH values, the application of this concept can therefore be used to probe abnormality. A repeat of the pH dependence property of the MOF in citric acid/NaOH system indicated that the MOF could be applied universally in different buffer systems within the pH range 3.00-7.00. In another development, Zheng et al [173] probed the connection between copper and Alzheimer's disease by using a MOF for the luminescent detection and removal of Cu from biological fluids despite the fact that copper concentrations therein are in trace amount. For the series of metals evaluated, Mg^{2+} and Cd^{2+} were found to increase the luminescence intensity compared to decrease by Mn^{2+}, Zn^{2+}, Ni^{2+}, and Co^{2+} cations whereas Cu^{2+} quenched the luminescence indicating that the presence of copper ions could be detected by the quenching of the luminescence. Further investigations indicated that the detection limit of this probe could reach 5 ppm and the photoluminescence showing an inverse relation to the concentration of Cu^{2+} ions. The facile nature of the Cu ions to get coordinated meant that in the presence of other ions, copper ions were selectively bound to the MOF ligand as was confirmed by the absence of copper ions in solution. A similar study involving fluorescence quenching in which copper ions are involved has been carried by Zhao et al [176] using a robust luminescent Tb(III)-MOF with Lewis basic pyridyl sites. The report indicated the ability of the MOF to detect the presence of Cu ion in simulated body fluids as well as nitromethane. Parallel results of quenching by analyte have been obtained by Abdelhamid et al [177] reported on $La(L_2)(H_2O)$ MOF (L = 2,4,6-tri-p-carboxyphenyl pyridine) MOF for luminescence studies of different metal ions. Significant responses were observed in the cases of Fe(III) and Fe(II) where quenching of SUMOF- 7II due to Fe(III) revealed that the fluorescence emission of SUMOF-7II can be selectively turned off in the presence of Fe(III). SUMOF-7II has a higher selectivity for Fe(III) compared to Fe(II). Evaluation of the selectivity of the MOF towards selected amino acids (L-histidine, L-asparagine, L-glutamine, L-leucine, L-methionine and L-tryptophan) revealed that whereas the others enhanced the luminescence, L-tryptophan quenched the emission giving the MOF a probe potential for L-tryptophan. Likewise, Dang et al [178] have used a Eu-MOF as a selective fluorescent probe for Fe^{3+} detection in biological media through a cation-exchange approach. The introduction of the MOF into simulated body fluid resulted to fluorescence quenching (with the intensity increasing with the concentration of iron ions in solution) consequent upon cation exchange in conformity with results described by Zhao et al [27]. The enhancement of chemoluminescence by MIL-53(Fe) in the presence of luminol–H_2O_2 has been reported. Chemoluminescence intensity of the luminol-H_2O_2-MIL-53(Fe) system was found to be about 20 times larger than that of the luminol-H_2O_2 solution under similar experimental conditions, indicating the signal enhancement of the MOF while the insignificant difference in XRD pattern confirmed the MOF as being a catalyst. The MOF complex could further be used to detect glucose ranging was from 0.1 to 10 µM by coupling with GOx [179]. MIL-53(Fe) has also been used to catalyze the oxidation of biological molecules 3,3',5,5'-tetramethylbenzidine (TMB), o-phenylenediamine (OPD), and 1,2,3-trihydroxybenzene (THB) in the presence of H_2O_2 and the concentration of resulting Fe^{3+} species detected by colorimetric methods. The catalytic activity of MIL-53(Fe) was found to be dependent on the pH, temperature, H_2O_2 concentration, and catalyst concentration with optimal conditions observed at approximately pH 4.0, 40 ^oC, and 480 µM H_2O_2. The catalytic mechanism of MIL-53(Fe) was as well investigated by the detection of in situ-generated hydroxyl radicals and glucose by means of photoluminescence method and results indicated a gradual increase in intensity with increasing MIL-53(Fe) concentration beginning with no intensity in the absence of MIL-53(Fe) [180–182]. Comparable reports [183,184] have posited the development of simple and sensitive colorimetric assay to detect H_2O_2 and ascorbic acid using an iron based MOF. As a result of the inherent peroxidase properties of both Fe(III)-based MOFs, a colorimetric technique for detection of H_2O_2 was established and used to quantitatively evaluate the amount of H_2O_2. MIL-68 and MIL-100 have equally been found to catalyze the oxidation of other peroxidase substrates such as OPD in the presence of H_2O_2, presenting a notable color. This oxidation process can be inhibited by the introduction of trace amount of ascorbic acid. Elsewhere Yin et al [185] on the other hand rather used a protein based MOF for peroxidase-like catalytic activity and colorimetric biosensing platform for the fast and sensitive detection of hydrogen peroxide and phenol. The protein-embedded ZIF-8@BHb hybrid MOF made using bovine hemoglobin (BHb) as the organic component and zeolitic imidazolate framework-8 (ZIF-8) as the inorganic component via self-assembly exhibited good stability and high catalytic activity for the oxidation of phenol and the detection of H_2O_2 during which a gradual change in color of the solution form colorless to red with limit of detection (LOD) of H_2O_2 by the naked-eye visualization to as low as 1 µM. Yang et al [186] recently developed a MOF that can be used as fluorescent sensor for human immunodeficiency virus 1 double-stranded DNA and Sudan virus RNA sequences respectively, with detection limits of 196 and 73 pM, respectively. The obtained MOF possessed channels which have aromatic ring, positively charged pyridinium and unsaturated Cu(II) cation centers, free carboxylates tessellating water and sulfate on the pore surface. This structure was found facilitate the formation of electrostatic, π-stacking,

and/or hydrogen-bonding interactions with two different carboxyfluorescein (FAM)-labeled probe ss-DNA to form two PDNA@ MOF systems; 5′-FAM-TTCTTCTTTTTTCT-3′ (P-DNA-1), a complementary sequence of HIV ds-DNA, and 5′-FAMTTAAAAAGTTTGTCCTCATC-3′ (P-DNA-2), a complementary sequence of Sudan virus RNA (SUDV RNA), respectively upon adding the MOF unto a solution of the PDNA. The combination of copper ions with the FAM led to the quenching of fluorescence. The introduction of a relevant target HIV ds-DNA sequences to the P-DNA-1@MOF system led to the formation of rigid triplex structure via reverse Hoogsteen base pairing while the introduction of complementary SUDV RNA sequences may lead to the formation of stable DNA/RNA hybrid duplex with PDNA-2. The formation of the rigid triplex or stable DNA/RNA hybrid forces the PDNA from the surface of the MOF and leads to the recovery of luminescence. Further investigations revealed that the channels of the MOFs play a critical role in distinguishing RNA from DNA. These results were consistent with that reported by Chen and coworkers [187].

Beyond luminescent approach to MOFs as already stated above, there have also emerged reports in which the electrochemical properties of MOFs have been employed for developing sensing probes. The electrochemical impedance spectroscopy can usually be used to monitor the surface properties of an electrode (whose surface is modified usually with a MOF) such as impedance, the capacity of the electrical double-layer, and charge transfer resistance. Consequently, any small change on the electrode surface could be detected to reveal the interactions or conformational changes of biomolecules [188]. In this light, Liu et al [188] recently reported on the pore modulation of Zr-MOF for huge efficiency detection of trace protein lysozyme. The surface of the electrode was modified using the MOF and used to immobilize aptamer strands on the electrode surface so that electron access and transfer was restrained. The introduction of this functionalized electrode into a solution containing lysozyme led to the a further blocking of the surface of the electrode and a continuous decrease of electrochemical activity and thus an increase of charge transfer resistance R_{ct} value as a result of the fact that the lysozyme bound to the aptamer. Further investigations with regards to selectivity of the electrode using familiar interference proteins such as platelet derived growth factor-BB (PDGF-BB), bovine serum albumin (BSA), thrombin, immunoglobulin G (IgG) and immunoglobulin E (IgE) indicated negligible increase of impedance by the interference proteins, which was attributed to the nonspecific sorption of these interference proteins by aptamers bound to the MOF on the electrode surface. The system could also be used to suitably detect real samples in human serum, wine and eggs. Wu et al [189] surface functionalize a glass-carbon electrode with $\{[Cu_2(HL)_2\text{-}(\mu_2\text{-}OH)_2(H_2O)_5]\cdot H_2O\}_n$ (H_2L = 2,5-dicarboxylic acid-3,4-ethylene dioxythiophene) for use as a biosensor in the simultaneous detection of ascorbic acid AA and L-tryptophan (L-Trp) from both a single-component solution and a bio-mimic environment. Electrochemical analysis revealed that the current density of the oxidation peak increases gradually with increase in the concentration of AA in the range 0.25 mM to 1.5 mM due to the absorption and subsequent interaction with the active sites of AA molecules unto the surface of the MOF. This selectivity of the MOF coated electrode toward AA in the presence of other interferents amino acids including L-alanine, D-alanine, L-glutamine, L-tryptophan, L-histidine, L-aspartic acid, L-proline, D-proline, L-tyrosine, L-cysteine, L-serine, L-lysine, L-threonine, DL-isoleucine, D-valine and L-arginine further confirmed the efficiency of the MOF in the detection of AA. Liu et al [190] developed and ultrasensitive immunoassay Au NPs and MOFs (Au-MOFs) composite to label the signal antibody (Ab2) by immobilizing Pt-covalent organic frameworks immobilized with capture antibodies (Ab1) to facilitate the signal amplification using C-reactive protein (CRP) as analyte. The presence of the Pt-COFs on the surface of the electrode decreased the electrochemical impedance while upon the introduction of target antigen CRP, the impedance increased due to antibody−antigen interaction. It has been explained that the capture of the MOF on the surface of the electrode is responsible for the increased impedance. One pot encapsulation of iron(III) meso-5,10,15,20-tetrakis(4-carboxyphenyl) porphyrin chloride (FeTCPP) into a prototypal MOF, HKUST-1[Cu] (and sequential conjugation with streptavidin as a recognition element) as mimetic catalysts for electrochemical DNA sensing via allosteric switch of hairpin DNA has been reported. The authors built on the fact that once activated, the hairpin DNA can selectively bind to FeTCPP @ MOF-SA via biorecognition affinity between streptavin SA, aptamer and SA and act as catalyst to enhance peroxidase activity toward o-phenylenediamine (OPD) oxidation in the presence of H_2O_2. The occurrence of large current peaks at -0.55 V corresponding to the allosteric switch from hairpin DNA to SA aptamer confirmed the effectiveness of the system in detecting the target DNA. The facilitation of diffusion of OPD in the electrochemical system was credited to the porous nature of the MOF. Further investigations using several DNA sequences revealed the high specificity of the system as a good biosensor mainly due to specific dual biorecognition of DNA hybridization and the aptamer affinity [191].

5.4 BioMOFs

In the application of MOFs as DDS, it is hypothesized that, once the MOF reaches the target site, the active ingredient is released either through diffusion and drug-matrix interaction or by means of framework disintegration. It is however worth noting that the disintegration of framework could release material which becomes problematic to the body. Mitigating or avoiding this phenomenon is essential to the successful application of MOFs in biological systems. It is within this context that the concept of BioMOFs has emerged where research seeks to synthesize and /or functionalize MOFs with biologically active ingredients. The fact that some metal cations such as Ca, Fe, Zn, Mg are biologically active implies that knowledge guided research could lead to MOFs wherein the body is under no pressure of eliminating any of the components as they are biologically relevant. Owing to the fact that most biological molecules might not form stable MOFs, design and synthesis of such materials in some cases has employed some non-biological ligands to enhanced stability. For such MOFs, porosity is not fundamental to their successful application since the active ingredient is part of the structure although it could be exploited for the purpose of co-delivery. Proteins, amino acids, peptides, nucleobases, carbohydrates, porphyrins and other therapeutic molecules such as nicotinic acid, deferiprone have been reportedly used as ligands in the synthesis of various BioMOFs [139,192]. These molecules may either be used as the building units or post synthesis. [193]. The flexibility and weak coordination ability of many biomolecules makes it difficult for such structures to crystalize into permanent porous framework necessitating the use of additional ligands in combination to increase their dimensionality and rigidity so that accessing the pores is facilitated [194,195]. Burrows et al [195] reported on incorporation by coordination and release of the iron chelator drug deferiprone (used to treat haemosiderosis and Alzheimer's disease) from zinc-based metal–organic frameworks. Elshwhere BioMOFs of well-known natural coloring pigment and food additive curcumin derived from turmeric has been reported [194]. It is also known to have therapeutic properties including anti-oxidative activity, anti-inflammatory activity, anticancer

activity, anti-HIV activity. Ibuprofen has been successfully loaded into the pores as confirmed by IR and TGA measurement. The release profile showed a two-step process, the second involving the breakdown of the MOF structure. Further investigation on MOFs on the basis of this ligand should prove useful. Levine et al [196] employed the anticancer drug olsalazine (H_4olz) as a ligand to synthesize a new series of mesoporous metal-organic frameworks that are expanded analogues of the familiar M_2(dobdc) materials (dobdc^{4-} = 2,5-dioxido-1,4-benzenedicarboxylate; M-MOF-74). The obtained MOFs exhibited the highest Langmuir surface areas among bioactive frameworks with pore apertures of approximately 27 Å, corresponding to the mesoporous range (≥20 Å). Olsalazine loading using the Mg based MOF reached 86% with a gradual release observed in PBS at physiological pH 7.4. Co-delivery of olsalazine and phenethylamine (PEA) was also studied and result indicated that over 90 wt % of the Mg_2(olz)$(PEA)_2$ MOF, material consists of a therapeutic organic molecule, with PEA and olsalazine accounting for 41 and 51 wt %, respectively with the PEA released more rapidly than the olsalazine linker. Additionally, the Fe_2(olz) framework could be fine-tuned to deliver anionic drugs by oxidizing to cationic Fe(olz)$^{2+}$. Lu et al. [197] reported on the solvothermal green synthesis of Na-β-cyclodextrin MOF. This MOF showed enhanced 5-FU loading (23.01%) compared to 15.73% for the pure ligand indicating the potential of the MOF as a DDS. Similar experiments by Li et al [198] obtained γ-CD based MOF and used it to encapsulate photochemical and electrochemical active fullerene (C_{60}). The authors found that the incorporation of C_{60} caused a reduction in the pore volumes of the pores ranging from 1.1 to 1.6 nm in diameter which were subsequently employed in the delivery studies of anticancer drug doxorubicin (DOX). Another cyclodextrin based MOF capable of encapsulating aqueous soluble guests, such as Rhodamine B by co-crystallization has been reported by Forgan et al. [199] with the metal-ligand ratio 1:8 using various alkaline earth and alkali metals. The inability to form transition metal MOFs of the cyclodextrin was attributed to the fact that coordination bonds from the protonated hydroxyl groups of γ-CD to the metal are not favored. Peptide-Zn MOFs obtained by reacting β-alanyl-L-histidine chain ligand, carnosine and zinc salt in DMF have been reported. The 3D purely microporous Zn-Car·DMF MOF showed structural flexibility and exhibited permanent porosity with BET surface area of 448 m^2g^{-1} and pore volume of 0.19 cm^3 g^{-1}upon DMF removal [200]. Similarly, water stable dinuclear chiral and homochiral MOFs with coordinative unsaturated metal sites and bridging AA (L-alanine, L-valine and L-leucine) bis(tridentate) ligands has been reported [200,201]. An et al [193] exploited the use of larger zinc-adeninate vertices and biphenyldicarboxylate BPDC to obtain mesoporous MOFs. The non-interpenetrating low density and high surface area MOF demonstrated hexagonal topology in the AB plane where the adjacent layers are displaced along the [110] direction leading to an ABAB 3D pattern along the c axis. Radford et al [202] have described Zn and Ni based protein self-assembly PSA MOFs occurring under thermodynamic control and the simultaneous incorporation of inorganic functionalities into multi-protein assemblies and frameworks. The surface of this metal binding protein phenanthroline (MBPPhen2) were accessible from the solvent channels, but however protected enough to potentially display selectivity. Similar reports by Broomell et al [203] have used protein cage nanoparticles as secondary building blocks to obtain non-interpenetrating network protein coordination polymers. Gas sorption studies of the MOF revealed that the material reversibly adsorbed CO_2 at 22 ^oC and 0^oC up to1.7 and 1.9 mmol g^{-1} at 20 bar, respectively. In a separate development, Sontz et al [204] have obtained cage-like octahedral symmetry MOFs using the highly stable human heavy-chain protein ferritin by means of vapor diffusion in the presence of excess $ZnCl_2$ at a pH 8.5. The bdh-Zn-T122H ferritin crystals demonstrated a high permeability to solutes, so that the ferritin hubs accomplished their natural enzymatic activity within the lattice, when oxidation of soluble Fe^{2+} into crystalline Fe^{3+}-oxide mineral occurred. Cai et al [199] have reported on a highly emissive and stable zinc(II) mixed ligand (adenine and benzene-1,3-dicarboxylate) solvo-thermal stable MOF with good host–guest chemopalette interaction for approaching white-light-emission. The introduction of acriflavine fluorescent molecules into the porous MOF prompted the improvement of light emission efficiency and control emission color of ZnBDCA. The authors found that, the intensity ratio of the host and guest can be changed exciting the MOF-acriflavine at different wavelengths, thereby changing the emission color from blue to yellow. Satter and Athar [205] [205] obtained a Copper glycinate (Bio-MOF-29) and further evaluated it in vitro adsorption studies of four different drugs; terazosine hydrochloride, telmisartan, glimpiride and rosuvastatin. HPLC, TGA and XRD were employed to establish and quantify the loading of drug molecules into the MOF. The slow release of adsorbed drugs after intervals was confirmed by means of HPLC. Liu et al [194] have reported on nanoscale hafnium-porphyrin MOF for combined photodynamic and radiation therapy in cancer treatment. The PEGylated NMOF showed greater singlet oxygen production compared to the prophyrin ligand upon exposure to a 661 nm laser at the power density of 5 mW/cm^2, attributed to the presence of heavy Hf^{4+} which facilitates the intersystem crossing of porphyrin ligand from the ground state to the excited state and the unique structure of NMOFs in which the photosensitizers are well isolated in the framework to avoid agglomeration and self-quenching of the excited states. Dual photodynamic and radiotherapy investigation revealed high effectiveness compared to using both approaches in isolation.

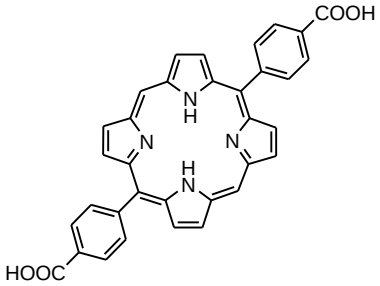

Figure 27: Structure of the porphyrin used obtain MOF [194]

Lu et al [206] in the same light reported on the rational design of a Hf-porphyrin nanoscale metal–organic framework, DBP–UiO, as an exceptionally effective photosensitizer for PDT of resistant head and neck cancer by incorporation of a porphyrin-derived bridging ligand into a robust and porous UiO NMOF structure with proper morphologies and dimensions. Investigation showed that the as-synthesized MOF is an excellent singlet oxygen generator. In vivo experiments on SQ20B subcutaneous xenograft murine models were used to evaluate the PDT efficacy of DBP–UiO and a 50 times tumor volume reduction in half of the mice and complete tumor eradication in the other half of the mice upon treatment with the DBP– UiO.

6. Conclusion

This review has examined current approaches to synthesis and post-synthetic modification of metal organic frameworks especially at nanoscale. With respect to biological applications, significant research has been carried out with promising results from success in synthesis to functionalization and applications. Given the vast reservoir of possible starting materials, various

synthetic approaches and attractive properties, MOFs hold a great potential in unlimited biological applications. Knowledge and application based synthetic approaches are paramount to the success of MOFs in biological applications.

Although many reports have shown interesting results in applications such as delivery of biological cargoes, the synthetic approaches of MOFs in most cases have had to deal with chemicals which for some are or could cause harm to the cells. Developing more biofriendly approaches to MOFs for these applications should therefore continue to be an active research area. Moreover, at nanoscale, MOFs are definitely more likely to be very attractive for applications inside biological systems but also possess improved sensitivity when it comes to biosensing. While this nanoscale approach and PSM may be able to escape barriers such as the complicated blood brain barriers, to deliver a cargo, the complications of retrieving the end product from such destinations must be clearly evaluated against an intended outcome since the end product possess properties markedly different from the initial MOF.

Author Biography

Baa Ebenezer received his BSc. and MSc. in chemistry from the University of Buea in Cameroon in 2008 and 2012 respectively and thereafter taught the subject at high school. He is currently a PhD student at Rhodes University where he is focusing on the synthesis and applications of MOFs for drug delivery under the supervision of Profs. Watkins, Krause, and Ndinteh.

GM Watkins is a professor in inorganic chemistry at Rhodes University with research interest in Metal Organic Framework materials (MOF's), bioinorganic metal complexes and ligand isotope studies of transition metal complexes for various application including but not limited to catalysis gas storage and biological applications.

Rui WM Krause is a leading researcher in Medicinal Chemistry and Nanomaterials. His work spans across drug-delivery, stimuli-responsive materials and renewable energy applications. He is currently also the head of department of chemistry at Rhodes University, South Africa.

Derek Ndinteh Tantoh is an associate professor of chemistry at the University of Johannesburg, South Africa. His research interest include; applications of synthetic and naturally occurring heterocycles, nano medicine and intelligent drug delivery systems.

References

[1] Furukawa H, Cordova K E, O'Keeffe M and Yaghi O M 2013 The Chemistry and Applications of Metal-Organic Frameworks *Science (80-.).* **341** 1–12

[2] Sun Y and Zhou H-C 2015 Recent progress in the synthesis of metal-organic frameworks *Sci. Technol. Adv. Mater.* **16** 054202

[3] Jambovane S R, Nune S K, Kelly R T, Mcgrail B P, Wang Z, Nandasiri M I, Katipamula S, Trader C and Schaef H T 2016 Continuous, One-pot Synthesis and Post-Synthetic Modification of NanoMOFs Using Droplet Nanoreactors *Nat. Publ. Gr.* **6** 1–9

[4] Moon H R, Lim D-W and Suh M P 2013 Fabrication of metal nanoparticles in metal-organic frameworks *Chem. Soc. Rev.* **42** 1807–24

[5] Orellana-Tavra C, Baxter E F, Tian T, Bennett T D, Slater N K H, Cheetham A K and Fairen-Jimenez D 2015 Amorphous metal-organic frameworks for drug delivery *Chem. Commun.* **51** 13878–81

[6] Bennett T D and Cheetham A K 2014 Amorphous Metal–Organic Frameworks *Acc. Chem. Res.* **47** 1555–1562

[7] Yang F, Li W and Tang B 2018 Facile synthesis of amorphous UiO-66 (Zr-MOF) for supercapacitor application *J. Alloys Compd.* **733** 8–14

[8] Beg S, Rahman M, Jain A, Saini S, Midoux P, Pichon C, Ahmad F J and Akhter S 2017 Nanoporous metal organic frameworks as hybrid polymer-metal composites for drug delivery and biomedical applications *Drug Discov. Today* **22** 625–37

[9] Liu R, Yu T, Shi Z and Wang Z 2016 The preparation of metal-organic frameworks and their biomedical application *Int. J. Nanomedicine* **11** 1187–200

[10] Kojtari A and Ji H 2015 Metal Organic Framework Micro/Nanopillars of Cu(BTC)·3H2O and Zn(ADC)·DMSO *Nanomaterials* **5** 565–76

[11] Janiak C, Vieth J K, Janiak C and Vieth J K 2010 MOFs, MILs and more: concepts, properties and applications for porous coordination networks (PCNs) *New J. Chem.* **34** 2366

[12] Zhang M, Bosch M, III T G and Zhou H-C 2014 Rational design of metal-organic frameworks with anticipated porosities and functionalities *CrystEngComm* **16** 4069–83

[13] Čejka J 2012 Metal-Organic Frameworks. Applications from Catalysis to Gas Storage. *Angew. Chemie Int. Ed.* **51** 4782–3

[14] Yaghi O. M L H 1995 Hydrothermal Synthesis of a Metal-Organic Framework Containing Large Rectangular Channels *J. Am. Chem. Soc.* **117** 10401–2

[15] Li H, Eddaoudi M O and Y O M 1999 Design and synthesi of an exceptionally stable and highly porous metal-organic framework *Nature* **402** 276–9

[16] Schoedel A and Yaghi O M 2016 Porosity in Metal – Organic Compounds *Macrocyclic and Supramolecular Chemistry: How Izatt-Christensen Award Winners Shaped the Field* ed Izatt Reed M. (Wiley and Sons, Ldt) pp 200–19

[17] Riou D and Ferey G 1998 Hybrid open frameworks (MIL-n). Part 3: Crystal structures of the HT and LT forms of MIL-7: a new vanadium propylenediphosphonate with an open-framework. Influence of the synthesis temperature on the oxidation state of vanadium within the same structural *J. Mater. Chem.* **8** 2733–5

[18] Yaghi O M, Li H, Eddaoudi M and O'Keeffe M 1999 No Title *Nature* **402** 276–9

[19] Keskin S and Seda K 2011 Biomedical Applications of Metal Organic Frameworks *Ind.Eng.Chem.Res.* **50** 1799–812

[20] Keskin S and Seda K 2011 Biomedical Applications of Metal Organic Frameworks *Ind. Eng. Chem. Res.* **50** 1799–812

[21] Rijnaarts T, Mejia-ariza R, Egberink R J M, Roosmalen W Van and Huskens J 2015 Metal-Organic Frameworks (MOFs) as Multivalent Materials: Size Control and Surface Functionalization by Monovalent Capping Ligands *Chem. Eur. J.* **21** 10296–301

[22] Sanchez A C 2014 *A New Synthetic Method for Nanoscale Metal-Organic Frameworks and their Application as Contrast Agents for Magnetic Resonance Imaging* (Authonomous University of Barcelona)

[23] Carne-Sanchez A, Imaz I, Cano-Sarabia M and Maspoch D 2013

Most studies have concentrated on whether a MOF performs a specific job or not at the neglect of the end life of the MOF; while this may be understandable for the fact that compared to the other materials, MOFs are new in the biological field, research must also be furthered to understand the fate of any MOF material once it has achieved an intended purpose. Finally, with research understandably gradually shifting to BioMOFs, care must be taken not to completely assess this class of materials from the properties of individual precursor components as this may be misleading. This is due to the fact that once the precursors are combined in a MOF the resultant observed properties may not always be the sum of properties of individual components. Holistic investigation is therefore paramount to the success of MOFs in biology.

Conflict of Interest

The authors have declared that no conflicting interest exist

A spray-drying strategy for synthesis of nanoscale metal-organic frameworks and their assembly into hollow superstructures *Nat. Chem.*

[24] Rocca J Della, Liu D and Lin W 2011 Nanoscale Metal Organic Frameworks for Biomedical Imaging and Drug Delivery *Acc. Chem. Res.* **44** 957–68

[25] Flügel E A, Ranft A, Haase F and Lotsch B V. 2012 Synthetic routes toward MOF nanomorphologies *J. Mater. Chem.* **22** 10119–10133

[26] Carné A, Carbonell C, Imaz I and Maspoch D 2011 Nanoscale metal-organic materials *Chem. Soc. Rev.* **40** 291–305

[27] Zhao H-X, Zou Q, Sun S-K, Yu C, Zhang X, Li R-J and Fu Y-Y 2016 Theranostic metal-organic framework core-shell composites for magnetic resonance imaging and drug delivery *Chem. Sci.* **7** 5294–301

[28] Yang Y, Wang F, Yang Q, Hu Y, Yan H, Chen Y Z, Liu H, Zhang G, Lu J, Jiang H L and Xu H 2014 Hollow metal-organic framework nanospheres via emulsion-based interfacial synthesis and their application in size-selective catalysis *ACS Appl. Mater. Interfaces* **6** 18163–71

[29] Rieter W J, Taylor K M L, An H, Lin W and Lin W 2006 Nanoscale Metal - Organic Frameworks as Potential Multimodal Contrast Enhancing Agents *J. Am. Chem. Soc.* **128** 9024–5

[30] Rieter W J, Taylor K M L, An H, Lin W and Lin W 2006 Nanoscale Metal-Organic Frameworks as Potential Multimodal Contrast Enhancing Agents. *J. Am. Chem. Soc.* **128** 9024–5

[31] Seoane B, Dikhtiarenko A, Mayoral A, Tellez C, Coronas J, Kapteijn F and Gascon J 2015 Metal organic framework synthesis in the presence of surfactants: towards hierarchical MOFs? *CrystEngComm* **17** 1693–700

[32] Tian C, Zhu L, Lin F and Boyes S G 2015 Poly(acrylic acid) Bridged Gadolinium Metal−Organic Framework−Gold Nanoparticle Composites as Contrast Agents for Computed Tomography and Magnetic Resonance Bimodal Imaging *ACS Appl. Mater. Interfaces* **7** 17765−17775

[33] Cao X, Dai L, Wang L, Liu J and Lei J 2015 A surfactant template-assisted strategy for synthesis of ZIF-8 hollow nanospheres *Mater. Lett.* **161** 682–5

[34] Zheng W, Hao X, Zhao L and Sun W 2017 Controllable Preparation of Nanoscale Metal-Organic Frameworks by Ionic Liquid Microemulsions *Ind. Eng. Chem. Res.* **56** 5899–905

[35] Tsuruoka T, Kumano M, Mantani K, Matsuyama T, Miyanaga A, Ohhashi T, Takashima Y, Minami H, Suzuki T, Imagawa K and Akamatsu K 2016 Interfacial Synthetic Approach for Constructing Metal − Organic Framework Crystals Using Metal Ion-Doped Polymer Substrate *Cryst. Growth Des.* **16** 2472–6

[36] Kim J, Min K, Noh H, Kim D, Park S and Kim P 2016 Direct Fabrication of Free-Standing MOF Superstructures with Desired Shapes by Micro-Confined Interfacial Synthesis. *Angew. Int. Ed.* **55** 7116–20

[37] Lu H and Zhu S 2013 Interfacial Synthesis of Free Standing Metal-Organic Frmaework Membranes *Eur. J. Inorg. Chem.* 1294–300

[38] Huang H, Li J, Wang K, Han T, Tong M, Li L, Xie Y, Yang Q, Liu D and Zhong C 2015 An in situ self-assembly template strategy for the preparation of hierarchical-pore metal-organic frameworks *Nat. Commun.* **6** 1–8

[39] Liu Y, Li H, Han Y, Lv X, Hou H and Fan Y 2012 Template-Assisted Synthesis of Co, Mn-MOFs with Magnetic Properties Based on Pyridinedicarboxylic Acid *Cryst. Growth Des.* **12** 3505−3513

[40] Sun L, Li J, Park J and Zhou H 2012 Cooperative Template-Directed Assembly of Mesoporous Metal − Organic Frameworks *J. Am. Chem. Soc.* **134** 126−129

[41] Peng L, Zhang J, Li J, Han B, Xue Z and Yang G 2012 Surfactant-directed assembly of mesoporous metal-organic framework nanoplates in ionic liquids *Chem. Commun.* **48** 8688–8690

[42] Qiu L, Li Z, Wu Y, Wang W, Xu T and Jiang X 2008 Facile synthesis of nanocrystals of a microporous metal–organic framework by an ultrasonic method and selective sensing of organoamines. *Chem. Commun.* 3642–4

[43] Choi J Y, Kim J, Jhung S H, Kim H, Chang J and Chae H K 2006 Microwave Synthesis of a Porous Metal-Organic Framework , Zinc Terephthalate MOF-5 *Bull. Korean Chem. Soc.* **27** 1523–4

[44] Lin Z, Yang Z, Liu T, Huang Y and Cao R 2012 Microwave-Assisted Synthesis of a Series of Lanthanide Metal-Organic Frameworks and Gas Sorption Properties *Inorg. Chem.* **51** 1813−1820

[45] Bag P P, Wang X and Cao R 2015 Microwave-assisted large scale synthesis of lanthanide metal-organic frameworks (Ln-MOFs), having a preferred conformation and photoluminescence properties *Dalt. Trans.* **44** 11954–62

[46] Taylor-pashow K M L, Rocca J Della, Xie Z, Tran S and Lin W 2009 Post-Synthetic Modifications of Iron-Carboxylate Nanoscale Metal-Organic Frameworks for Imaging and Drug Delivery *J. Am. Chem. Soc.* **131** 14261–3

[47] Masoomi M Y and Morsali A 2016 Sonochemical synthesis of nanoplates of two Cd (II) based metal-organic frameworks and their applications as precursors for preparation of nanomaterials *Ultrason. Sonochem.* **28** 240–9

[48] Karizi F Z, Safarifard V, Khani S K and Morsali A 2015 Ultrasound-assisted synthesis of nano-structured 3D zinc (II) metal-organic polymer: Precursor for the fabrication of ZnO *Ultrason. - Sonochemistry* **23** 238–45

[49] Bigdeli M and Morsali A 2015 Ultrasonics Sonochemistry Sonochemical synthesis of a nano-structured zinc(II) amidic pillar metal-organic framework *Ultrason. - Sonochemistry* **27** 416–22

[50] Bigdeli F, Ghasempour H, Tehrani A A, Morsali A and Hosseini-monfared H 2017 Ultrasound-Assisted Synthesis of Nano-Structured Zinc (II)-Based Metal-Organic Frameworks as Precursors for the synthesis of ZnO nanostructure *Ultrason. - Sonochemistry* **37** 29–36

[51] Haque En, Khan N A, Park J H and Jhung S H 2010 Synthesis of a Metal-Organic Framework Material, Iron Terephthalate, by Ultrasound, Microwave. *Chem. Eur. J.* **16** 1046 – 1052

[52] Ata-ur-Rehman, Tirmizi S A, Badshah A, Ammad H M, Jawad M, Abbas S M, Rana U A and Khan S U-D 2017 Synthesis of Highly Stable MOF-5@MWCNTs nanocomposites with Improved Hydrophobic Properties *Arab. J. Chem.*

[53] Patil R, Pande V and Sonawane R 2015 Nano and Microparticulate Chitosan Based System for Formulation of Cardiovascular Rapid Melt Tablet *Adv. Pharm. Bull.* **5** 169–79

[54] Bhandari B ., Dumoulin E ., Richard H M J, Noleau I and Lebert A M 1992 Flavour Encapsulation by Spray Drying: Application to Citral and Linalyl Acetate *J. Food Sci.* **57** 217–21

[55] Carvalho A G S, Silva V M and Hubinger M D 2014 Microencapsulation by Spray Drying of Emulsified Green Coffee Oil with Two-layered Membranes *Food Res. Int.* **61** 236–45

[56] Rubio-Martinez M, Avci-Camur C, Thornton A W, Imaz I, Maspoch D and Hill M H 2017 New synthetic Routes Towards MOF Production at Scale *Chem. Soc. Rev.* **46** 3453–80

[57] Rivas-Murias B, Fagnard J F, Vanderbemden P, Traianidis M, Cloots C and Vetruyen B 2011 Spray-Drying: An atlternative Synthesis Method for Polycationic Oxide Compounds *J. Phys. Chem. Solids* **72** 158–63

[58] Garzón-Tovar L, Cano-Sarabia M, Carné-Sánchez A, Carbonell C, Imaz I and Maspoch D 2016 A spray-drying continuous-flow method for simultaneous synthesis and shaping of microspherical high nuclearity MOF beads *React. Chem. Eng.* **1** 533–9

[59] Guillerm V, Garzon-Tovar L, Yazdi A, Imaz I, Juanhuix J and Maspoch D 2017 Continous One-Step Synthesis of Porous M-XF6-Based Metal-organic and Hydrogen Frameworks *Eur. J. Chem.* **23** 6829–35

[60] Marquez A G, Horcajada P, Grosso D, Ferey G, Serre C, Sanchez C and Boissiere C 2013 Green Scalable Aerosl Syhthesis of Porous Metal-Organic Frameworks *Chem. Commun.* **49** 3848–50

[61] Klimakow M, Klobes P, Thunemann A F, Rademann K and Emmerling F 2010 Mechanochemical Synthesis of Metal-organic Frameworks: A Fast Facile Approach Toward Qunatitative Yields and High Specific Surface Areas *Chem. Mater.* **22** 5216–21

[62] Dey C, Kundu T, Biswal B P, Mallick A and Banerjee R 2014 Crystalline Metal-Organic Frameworks (MOFs): Synthesi, Structure and Function *Acta Crystallogr.* **B70** 2–10

[63] Yousefi M and Zeid S S 2016 mechnochemical Synthesis of Nano-Structured Copper(II) Metal Organic Framework as precursor for the Preparation of Copper Oxide Nanoparticles

Am. Chem. Sci. J. **15**

[64] Razaei M, Abbasi A, Varshochian R, Dinarvand R and Jeddi-Tehrani M 2017 NanoMIL-100(Fe) containing docetaxel for breast cancer therapy *Artif. Cells, Nanomedicine, Biotechnol.* **47** 1–12

[65] Peng Y, Li Y, Ban Y, Jin H, Jiao W, Liu X and Yang W 2014 Metal-organic framework nanosheets as building blocks for molecular sieving membranes *Chem. Commun.* **346**

[66] Foster J A, Henke S, Schneemann A, Roland F A and Cheetham A K 2016 Liquid exfoliation of alkyl-ether functionalised layered metal organic frameworks to nanosheets *Chem. Commun.* **52** 10474–7

[67] Zhao M, Lu Q, Ma Q and Zhang H 2017 Two-Dimensional Metal Organic Frameworks Nanosheets. *Small Methods* **1** 1–8

[68] Li W, Su P, Li Z, Xu Z, Wang F, Ou H, Zhang J, Zhang G and Zeng E 2017 Ultrathin metal-organic framework membrane production by gel-vapour deposition *Nat. Commun.* **8** 1–8

[69] Summerfield A, Cebula I, Schroder M and Beton P H 2015 Nucleation and Early Stages of Layer-by-Layer Growth of Metal Organic Frameworks on Surfaces *Joournal Phys. Chem.* **119** 23544–51

[70] Shekhah O, Wang H, Strunskus T, Cyganik P, Zacher D, Fischer R and Woll C 2007 Layer-by-Layer Growth of Oriented Metal Organic Polymers on a Functionalized Organic Surface *Langmuir* **23** 7440–2

[71] Laokroekkiat S, Hara M, Nagano S and Nagao Y 2016 Metal-Organic Coordination Network Thin Film by Surface-Induced Assembly *Langmuir* **32** 6648–55

[72] Shekhah O 2010 Layer-by-Layer Method for the Synthesis and Growth of Surface Mounted Metal-Organic Frameworks (SURMOFs) *Materials (Basel).* **3** 1302–15

[73] Liu J, Shekhah O, Stammer X, Arslan H K, Liu B, Schüpbach B, Terfort A and Wöll C 2012 Deposition of Metal-Organic Frameworks by Liquid-Phase Epitaxy: The Influence of Substrate Functional Group Density on Film Orientation *Materials (Basel).* **5** 1581–92

[74] Gui B, Meng X, Xu H and Wang C 2016 Postsynthetic Modification of Metal Organic Framework Through Click Chemistry *Chinese J. Chem.* **34** 186—190

[75] Hintz H and Wuttke S 2014 Postsynthetic modification of an amino-tagged MOF using peptide coupling reagents: a comparative study *Chem. Commun.* **50** 11472–5

[76] Wuttke S, Braig S, Preiß T, Zimpel A, Sicklinger J, Bellomo C, Radler J O, Vollmar bAngelika M and Bein T 2015 MOF nanoparticles coated by lipid bilayers and their uptake by cancer cells *Chem. Commun.* **51** 15752–5

[77] Molavi H, Eskandari A, Shojaei A and Mousavi S A 2018 Enhancing CO2/N2 adsorptioin selectivity via post synthetic modification of NH2-UiO-66(Zr) *Microporous Mesoporous Mater.* **257** 193–201

[78] Zhang X, Zhang J, Hu Q, Cui Y, Yang Y and Qian G 2015 Applied Surface Science Postsynthetic modification of metal-organic framework for hydrogen sulfide detection *Appl. Surf. Sci.* **355** 814–9

[79] Morris W, Doonan C J and Yaghi O M 2011 Postsynthetic Modification of a Metal-Organic Framework for Stabilization of a Hemiaminal and Ammonia Uptake *Inorg. Chem.* **50** 6853–5

[80] Tanabe K K, Wang Z and Cohen S M 2008 Systematic Functionalization of a Metal-Organic Framework via a Postsynthetic Modification Approach *J. Am. Chem. Soc.* **130** 8508–17

[81] Yang F, Yang C X and Yan X P 2015 Post-synthetic modification of MIL-101(Cr) with pyridine for high-performance liquid chromatographic separation of tocopherols *Talanta* **137** 136–42

[82] Yang B, Shen M, Liu J and Ren F 2017 Post-Synthetic Modif ication Nanoscale Metal- Organic Frameworks for Targeted Drug Delivery in Cancer Cells *Pharm. Res.* **34** 2440–50

[83] Köppen M, Beyer O, Wuttke S, Lüning U and Stock N 2017 Synthesis, functionalisation and post-synthetic modification of bismuth metal–organic frameworks *Dalt. Trans.* **46** 8658–63

[84] Gee W J, Cadman L K, Hamzah H A, Mahon M F, Raithby P R and Burrows A D 2016 Furnishing Amine-Functionalized Metal-Organic Frameworks with the β‑ Amidoketone Group by Postsynthetic Modification *Inorg. Chem.* **55** 10839–10482

[85] Aguilera-Sigalat J, Fox-Charles A and Bradshaw D 2014 Direct Photo-hydroxylation of the Zr-based framework UiO-66 *Chem. Commun.* **50** 15453–6

[86] DeCoste J B, Browe M A, Wagner G W, Rossin joseph A and Peterson G W 2015 Removal of Chlorine Gas by an Amine Functionalized Metal-Organic Framework via Electrophilic Aromatic Substitution *Chem. Commun.* **51** 12474–7

[87] Xu L, Luo Y, Sun L, Pu S, Fang M, Yuan R-X and Du H-B 2016 Turning the Properties of the Metal-Organic Framework UiO-67-bpy via Post-Synthetic N-Quaternization of Pyridine Sites *Dalt. Trans.* **45** 8614–21

[88] Qi Z, Jiancan Y, Jianfeng C, Ling Z, Yuanjing C, Yu Y, Banglin C and Qian G 2015 A Porous Zr-Cluster-Based Cationic Metal Organic Framework for Highly Efficient Cr2O72- Removal from Water *Chem. Commun.* **51** 14732–4

[89] Marshall R J, Griffin S L, Wilson C and Forgan R S 2016 Stereoselective Halogenation of Integral Unsaturated C-C Bonds in Chemically and Mechanically Robust Zr and Hf MOFs *Eur. J. Chem.* **22** 4870–7

[90] Marshall R J, Griffin S L, Wilson C and Forgan R S 2015 Single-Crystal to Single-Crystal Mechanical Contraction of Metal-Organic Frameworks through Stereoselcetive Postsynthetic Bromination *J. Am. Chem. Soc.* **137** 9527–30

[91] Marshall R J, Richards T, Hobday C L, Murphie C F, Wilson C, Moggach S A, Bennett T D and Forgan R S 2016 Post Synthetic Bromination of UiO-66 Analogues: Altering Linker Flexibility and Mechanical Compliance *Dalt. Trans.* **46** 4132–5

[92] Marshall Ross J and Forgan Ross S 2016 Post Synthetic Modification of Zirconium Metal Organic Frameworks *Eur. J. Inorg. Chem.* 4310–31

[93] Smith S J D, Konstas K, Lau C H, Gozukara Y M, Easton C D, Mulder R J, Ladewig B P and Hill M R 2017 Post-Synthetic Annealing: Linker Self-Exchange in UiO-66 and Its Effect on Polymer-Metal Organic Framework Interaction *Cryst. Growth Des.* **17** 4384−4392

[94] Karagiaridi O, Bury W, Mondloch J E, Hupp J T and Farha O K 2014 Solvent-Assisted Linker Exchange: An Alternative to the De Novo Synthesis of Unattainable Metal–Organic Frameworks *Angwandte chemie nternational Ed.* **53** 4530–40

[95] Gadipelli S and Guo Z 2014 Postsynthesis Annealing of MOF-5 Remarkably Enhances the Framework Structural Stability and CO2 Uptake *Chem. Mater.* **26** 6333−6338

[96] Burnett B J, Barron P M, Hu C and Choe W 2011 Stepwise Synthesis of Metal Organic Frameworks: Replacement of Structural Organic Linkers *J. Am. Chem. Soc.* **133** 9984–7

[97] Islamoglu T, Goswami S, Li Z, Howarth A J, Farha O K and Hupp J T 2017 Postsynthetic Tuning of Metal-Organic Frameworks for Targeted Applications *Acc. Chem. Res.* **50** 805−813

[98] Lau C H, Babarao R and Hill M R 2013 A route to drastic increase of CO2 uptake in Zr metal organic framework UiO-66 *Chem. Commun.* **49** 3634–7

[99] Fei H, Cahill J F, Prather K A and Cohen S M 2013 Tandem Postsynthetic Metal Ion and Ligand Exchange in Zeolitic Imidazolate Frameworks *Inorg. Chem.* **52** 4011–6

[100] Jiang J, Yang C and Yan X 2015 Postsynthetic ligand exchange for the synthesis of benzotriazole-containing zeolitic imidazolate framework *Chem. Commun.* **51** 6540–3

[101] Fluch U, Paneta V, Primetzhofer D and Ott S 2017 Uniform distribution of post-synthetic linker exchange in metal-organic frameworks revealed by Rutherford backscattering spectrometry *Chem. Commun.* **53** 6516–9

[102] Szilágyi P Á, Serra-Crespo P, Gascon J, Geerlings H and Dam B 2016 The impact of Post-synthetic linker Functionalization of MOFs on Methane storage: The role of Defects *Front. Energy Res.* **4**

[103] Boissonnault J A, Wong-foy A G and Matzger A J 2017 Core–Shell Structures Arise Naturally During Ligand Exchange in Metal–Organic Frameworks *J. Am. Chem. Soc.* **139** 14841–4

[104] Mcguire C V and Forgan R S 2015 The surface chemistry of metal-organic frameworks *Chem. Commun.* **51** 5199–217

[105] Larazo Isabel Abanades, Haddad Salame, Sacca Sabrina, Orellana-Tavra Claudia, Fairen-Jimenez David and F R S 2017 Selective Surface PEglation of UiO-66 Nanoparticles for Enhanced Stability, Cell Uptake and pH Responsive Drug Delivery *Chemistry (Easton).* **2** 561–78

[106] Rocca J Della, Liu D and Lin W 2013 Nanoscale Metal-Organic Frameworks for Biomedical Imaging and Drug Delivery *Acc. Chem. Res.* **44** 957–68

[107] Jung S and Park S 2017 Dual-Surface Functionalization of Metal-Organic Frameworks for Enhancing the Catalytic Activity of Candida antarctica Lipase B in Polar Organic Media *ACS Catal.* **7** 438−442

[108] Karagiaridi O, Bury W, Mondloch J E, Hupp J T and Farha O K 2014 Solvent-Assisted Linker Exchange: An Alternative to the De Novo Synthesis of Unattainable Metal-Organic Frameworks *Angew. Chemie Int. Ed.* **53** 4530–40

[109] Li Z and Zeng H C 2014 Armored MOFs: Enforcing Soft Microporous MOF Nanocrystals with Hard Mesoporous Silica *J. Am. Chem. Soc.* **136** 5631−5639

[110] Wang S, Morris W, Liu Y, McGuirk C M, Zhou Y, Hupp J T, Farha O K and Mirkin C A 2015 Surface-Specific Functionalization of Nanoscale Metal-Organic Frameworks *Angew. Chemie Int. Ed.* **54** 14738–42

[111] Zhao D, Tan S, Yuan D, Lu W, Rezenom Y H, Jiang H, Wang L-Q and Zhou H C 2011 Surface Functionalization of Porous Coordination Nanocages Via Click Chemistry and Their Application in Drug Delivery *Adv. Mater.* **23** 90–3

[112] Sun Q, He H, Gao W, Aguila B, Wojtas L, Dai Z, Li J, Chen Y, Xiao F and Ma S 2016 Imparting amphiphobicity on single-crystalline porous materials *Nat. Commun.* **7** 1–7

[113] Deria P, Mondloch J E, Karagiaridi O, Bury W, Hupp J T and Farha O K 2014 Beyond post-synthesis modification: evolution of metal–organic frameworks via building block replacement *Chem. Soc. Rev.* **43** 5896–912

[114] Deria P, Chung Y G, Snurr R Q, Hupp J T and Farha O K 2015 Water stabilization of Zr6-based metal-organic frameworks via solvent-assisted ligand incorporation *Chem. Sci.* **6** 5172–6

[115] Wu H, Chua Y S, Krungleviciute V, Tyagi M, Chen P, Yildirim T and Zhou W 2013 Unusual and Highly Tunable Missing-Linker Defects in Zirconium Metal-Organic Framework UiO-66 and Their Important Effects on Gas Adsorption *J. Am. Chem. Soc.* **135** 10525−10532

[116] DeCoste J B, Demasky T J, Katz M J, Farha O K and Hupp J T 2015 A UiO-66 analogue with uncoordinated carboxylic acids for the broad-spectrum removal of toxic chemicals *New J. Chem.* **39** 2396–9

[117] Katz M J, Brown Z J, Colon Y J, Siu P W, Scheidt K A, Snurr R Q, Hupp J T and Farha O K 2013 A facile synthesis of UiO-66, UiO-67 and their derivatives *Chem. Commun.* **49** 9449–51

[118] Rimoldi M, Nakamura A, Vermeulen N A, Henkelis J J, Blackburn A K, Hupp J T, Stoddart J F and Farha O K 2016 A metal–organic framework immobilised iridium pincer complex *Chem. Sci.* **7** 4980–4

[119] Dolgopolova E A, Ejegbavwo O A, Martin C R, Smith M D, Setyawan W, Karakalos S G, Henager C H, Loye H and Shustova N B 2017 Multifaceted Modularity: A Key for Stepwise Building of Hierarchical Complexity in Actinide Metal–Organic Frameworks *J. Am. Chem. Soc.*

[120] Yuan S, Lu W, Chen Y, Zhang Q, Liu T, Feng D, Wang X, Qin J and Zhou H 2015 Sequential Linker Installation: Precise Placement of Functional Groups in Multivariate Metal−Organic Frameworks *J. Am. Chem. Soc.* **137** 3177−3180

[121] Evans J D, Sumby C J and Doonan C J 2014 Post Synthetic Metalation of Metal Organic Frwamworks *Chem. Soc. Rev.* **43** 5933–51

[122] Kumar R M, Sundar J V and Subramanian V 2012 Improving the hydrogen storage capacity of metal organic framework by chemical functionalization *Int. J. Hydrogen Energy* **37** 16070–7

[123] Manna K, Zhang T and Lin W 2014 Postsynthetic Metalation of Bipyridyl-Containing Metal-Organic Frameworks for Highly Efficient Catalytic Organic Transformations *J. Am. Chem. Soc.* **136** 6566–6560

[124] Manna K, Zhang T, Greene F X and Lin W 2015 Bipyridine and Phenanthroline Based Metal-Organic Frameworks for Highly Efficient and Tandem Catalytic Organic Transformations via Directed C-H Activation *J. Am. Chem. Soc.* **137** 2665–73

[125] Zheng X, Fan R, Song Y, Wang A, Xing K, Du X, Wang P and Yang Y 2017 A highly sensitive turn-on ratiometric luminescent probe based on postsynthetic modification of Tb3+@Cu-MOF for H2S detection *J. Mater. Chem. C* **5** 9943–51

[126] Colón Y J, Fairen-jimenez D, Wilmer C E and Snurr R Q 2014 High-Throughput Screening of Mg-Functionalized Metal-Organic Frameworks for Hydrogen Storage near Room Temperature *J. Phys. Chem. C,* **118** 5383–9

[127] Fei H, Shin J, Meng Y S, Adelhardt M, Sutter J, Meyer K and Cohen S M 2014 Reusable Oxidation Catalysis Using Metal-Monocatecholato Species in a Robust Metal-Organic Framework *J. Am. Chem. Soc.* **136** 4965–73

[128] Li B, Ma D, Li Y, Zhang Y, Li G, Shi Z, Feng S, Zaworotko M J and Ma S 2016 Dual Functionalized Cages in Metal-Organic Frameworks via Stepwise Postsynthetic Modification *Chem. Mater.* **28** 4781−4786

[129] Zhang J-P, Zhou H-L, Zhou D-D, Liao P-Q and Chen X-M 2017 Controlling flexibility of metal-organic frameworks *Natl. Sci. Rev.* **0** 1–13

[130] Kim Y, Haldar R, Kim H, Koo J and Kim K 2016 The guest-dependent thermal response of the flexible MOF Zn2(BDC)2(DABCO) *Dalt. Trans.* **45** 4187–92

[131] Phillips A E, Goodwin A L, Halder G J, Southon P D and Kepert C J 2008 Nanoporosity and exceptional negative thermal expansion in single-network cadmium cyanide *Angew. Chemie - Int. Ed.* **47** 1396–9

[132] Gao X, Zhai M, Guan W, Liu J, Liu Z and Damirin A 2017 Controllable Synthesis of a Smart Multifunctional Nanoscale Metal − Organic Framework for Magnetic Resonance / Optical Imaging and Targeted Drug Delivery *ACS Appl. Mater. Interfaces* **9** 3455−3462

[133] Choudhary E, Thakur P, Pareek M and Agarwal N 2015 Gene silencing by CRISPR interference in mycobacteria *Nat. Commun.* **6** 1–11

[134] Xiao J D, Han L, Luo J, Yu S H and Jiang H L 2018 Integration of Plasmonic Effects and Schottky Junctions into Metal-Organic Framework Composites: Steering Charge Flow for Enhanced Visible-Light Photocatalysis *Angew. Chemie - Int. Ed.* **57** 1103–7

[135] Yang Q, Xu Q, Yu S H and Jiang H L 2016 Pd Nanocubes@ZIF-8: Integration of Plasmon-Driven Photothermal Conversion with a Metal-Organic Framework for Efficient and Selective Catalysis *Angew. Chemie - Int. Ed.* **55** 3685–9

[136] Xiao J D, Shang Q, Xiong Y, Zhang Q, Luo Y, Yu S H and Jiang H L 2016 Boosting Photocatalytic Hydrogen Production of a Metal-Organic Framework Decorated with Platinum Nanoparticles: The Platinum Location Matters *Angew. Chemie - Int. Ed.* **55** 9389–93

[137] Zhang W, Lu G, Cui C, Liu Y, Li S, Yan W, Xing C, Chi Y R, Yang Y and Huo F 2014 A family of metal-organic frameworks exhibiting size-selective catalysis with encapsulated noble-metal nanoparticles *Adv. Mater.* **26** 4056–60

[138] Yang Q, Liu W, Wang B, Zhang W, Zeng X, Zhang C, Qin Y, Sun X, Wu T, Liu J, Huo F and Lu J 2017 Regulating the spatial distribution of metal nanoparticles within metal-organic frameworks to enhance catalytic efficiency *Nat. Commun.* **8** 1–9

[139] Rojas S, Devic T and Horcajada P 2017 Metal organic frameworks based on bioactive components *J. Mater. Chem. B* **5** 2560–73

[140] Li Y, Li X, Guan Q, Zhang C, Xu T, Dong Y, Bai X and Zhang W 2017 Strategy for chemotherapeutic delivery using a nanosized porous metal-organic framework with a central composite design *Int. J. Nanomedicine* **12** 1465–74

[141] Haydar M A L, Abid H R, Sunderland B and Wang S 2017 Metal organic frameworks as a drug delivery system for flurbiprofen *Drug Desig, Dev. Ther.* **11** 2685–95

[142] Yang Y, Hu Q, Zhang Q, Jiang K, Lin W, Yang Y, Cui Y and Qian G 2016 A Large Capacity Cationic Metal-Organic Framework Nanocarrier for Physiological pH Responsive Drug Delivery *Mol. Pharm.* **13** 2782–6

[143] Mckinlay A C, Allan P K, Renouf C L, Duncan M J, Wheatley P S, Warrender J, Dawson D, Ashbrook S E, Gil B, Marszalek B, Düren T, Williams J J, Charrier C, Mercer D K, Teat S J and Morris R E 2014 Multirate delivery of multiple therapeutic agents from metal-organic frameworks *APL Mater.* **124108** 1–8

[144] Zhang H, Jiang W, Liu R, Zhang J, Zhang D, Li Z and Luan Y 2017 Rational Design of Metal Organic Framework Nanocarrier-Based Codelivery System of Doxorubicin Hydrochloride/Verapamil Hydrochloride for Overcoming Multidrug Resistance with Efficient Targeted Cancer Therapy

ACS Appl. Mater. Interfaces **9** 19687–97

[145] Vasconcelos L D F 2012 *RGD-Based Metal Organic Frameworks For Selective Delivery Of Therapeutics To Tumour Vasculature* (PhD thesis submitted to the University of Porto)

[146] Rojas S, Wheatley P S, Quartapelle-Procopio E, Gil B, Marszalek B, Morris R E and Barea E 2013 Metal-Organic Frameworks as Potential Multi- Carriers of Drugs *Cryst. Eng. Commun.* **15** 9364–9367

[147] He C, Lu K, Liu D and Lin W 2014 Nanoscale Metal − Organic Frameworks for the Co-Delivery of Cisplatin and Pooled siRNAs to Enhance Therapeutic E ffi cacy in Drug-Resistant Ovarian Cancer Cells *J. Am. Chem. Soc.* **136** 5181–4

[148] Illes B, Wuttke S and Engelke H 2017 Liposome-Coated Iron Fumarate Metal-Organic Framework Nanoparticles for Combination Therapy *Nanomaterials* **351** 1–11

[149] Hu Q, Yu J, Liu M, Liu A, Dou Z and Yang Y 2014 A Low Cytotoxic Cationic Metal − Organic Framework Carrier for Controllable Drug Release *J. Med. Chem.* **57** 5679−5685

[150] An J, Geib S J and Rosi N L 2009 Cation-Triggered Drug Release from a Porous Zinc-Adeninate Metal-Organic Framework *J. Am. Chem. Soc.* **131** 8376–7

[151] Sun C, Qin C, Wang C, Su Z, Wang S, Wang X, Yang G, Shao K, Lan Y and Wang E 2011 Chiral Nanoporous Metal-Organic Frameworks with High Porosity as Materials for Drug Delivery *Adv. Mater.* **23** 5629–32

[152] Li Q, Wang J, Liu W, Zhuang X, Liu J, Fan G, Li B, Lin W and Man J 2015 A new (4,8)-connected topological MOF as potential drug delivery *Inorg. Chem. Commun.* **55** 8–10

[153] Luo Z, Wang R, Gu C, Li F, Han Y, Li B and Liu J 2017 A metal-organic framework with unusual nanocages: Drug delivery *Inorg. Chem. Commun.* **76** 91–4

[154] Gu C, Li F, Li B, Xu J, Yang S, Luo M, Liu J and Liu G 2016 Rational synthesis of a porous polyhedral metal-organic framework carrier for controllable drug release *Inorg. Chem. Commun.* **73** 26–9

[155] Ahmad N, Younus H A, Chughtai A H, Hecke K Van, Danish M, Gaoke Z and Verpoort F 2017 Development of Mixed metal Metal-organic polyhedra networks, colloids, and MOFs and their Pharmacokinetic applications *Sci. Rep.* **7** 1–8

[156] Orellana-tavra C, Marshall R J, Baxter E F, Lazaro I A, Tao A, Cheetham A K, Forgan R S and Fairen-Jimenez 2016 Drug delivery and controlled release from biocompatible metal-organic frameworks using mechanical amorphization *J. Mater. Chem. B* **4** 7697–707

[157] Tian Z, Yao X, Ma K, Niu X, Grothe J, Xu Q, Liu L, Kaskel S and Zhu Y 2017 Metal-Organic Framework/Graphene Quantum Dot Nanoparticles Used for Synergistic Chemo- and Photothermal Therapy *ACS Omega* **2** 1249–58

[158] Erucar I and Keskin S 2016 Efficient Storage of Drug and Cosmetic Molecules in Biocompatible Metal Organic Frameworks: A Molecular Simulation Study *Ind. Eng. Chem. Res.* **55** 1929−1939

[159] Cunha D, Yahia M Ben, Hall S, Miller S R, Chevreau H, Elkaim E, Maurin G, Horcajada P and Serre C 2013 Rationale of Drug Encapsulation and Release from Biocompatible Porous Metal-Organic Frameworks *Chem. Mater.* **25** 2767−2776

[160] Rojas S, Carmona F J, Maldonada C R, Barea E and Navarro J A 2015 RAPTA-C incorporation and controlled delivery from MIL-100 (Fe) nanoparticles *New J. Chem.* **100**

[161] Alsaiari S K, Patil S, Alyami M, Alamoudi K O, Aleisa F A, Merzaban J S, Li M and Khashab N M 2018 Endosomal Escape and Delivery of CRISPR/Cas9 Genome Editing Machinery Enabled by Nanoscale Zeolitic Imidazolate Framework *J. Am. Chem. Soc.* **140** 143–6

[162] Hemphill J, Borchardt E K, Brown K, Asokan A and Deiters A 2015 Optical Control of CRISPR / Cas9 Gene Editing *J. Am. Chem. Soc.* **137** 5642−5645

[163] Liao H, Gu Y, Diaz A, Marlett J, Takahashi Y, Li M, Suzuki K, Xu R, Hishida T, Chang C, Esteban C R, Young J, Carlos J and Belmonte I 2015 Use of the CRISPR/Cas9 system as an intracellular defense against HIV-1 infection in human cells *Nat. Commun.* **6** 1–10

[164] Rocca J Della, Liu D and Lin W 2011 Nanoscale Metal-Organic framework for Biomedical Imaging and Drug Delivery *Acc. Chem. Res.* **44** 957–68

[165] Miller S E, Teplensky M H, Moghadam P Z and Fairen-jimenez D 2018 Metal-organic frameworks as biosensors for luminescence-based detection and imaging *Interface Focus* **6** 1–14

[166] Gao X, Ji G, Cui R, Liu J and Liu Z 2017 In situ growth of metal-organic frameworks (MOFs) on the surface of other MOFs: a new strategy for constructing magnetic resonance/optical dual mode imaging materials *Dalt. Trans.* **46** 13686–9

[167] Deng K, Hou Z, Li X, Li C, Zhang Y, Deng X, Cheng Z and Lin J 2015 Aptamer-Mediated Up-conversion Core/ MOF Shell Nanocomposites for Targeted Drug Delivery and Cell Imaging *Sci. Rep.* **5** 1–7

[168] Wang Y, Liu W and Yin X 2017 Multifunctional mixed-metal nanoscale coordination polymers for triple-modality imaging-guided photodynamic therapy *Chem. Sci.* **8** 3891–7

[169] Horcajada P, Chalati T, Serre C, Gillet B, Sebrie C, Baati T, Eubank J F, Heurtaux D, Clayette P, Kreuz C, Chang J, Hwang Y K, Marsaud V, Bories P, Cynober L, Gil S, Férey G, Couvreur P and Gref R 2010 Porous metal–organic-framework nanoscale carriers as a potential platform for drug delivery and imaging *Nat. Mater.* **9** 172–8

[170] Lim Y T, Kim S, Nakayama A, Stott N E, Bawendi M G and Frangioni J V 2003 Selection of Quantum Dot Wavelengths for Biomedical Assays and Imaging *Mol. Imaging* **2** 50–64

[171] Frangioni J V 2003 In vivo near-infrared fluorescence imaging *Curr. Opin. Chem. Biol.* **7** 626–34

[172] Foucault-collet A, Gogick K A, White K A, Villette S, Pallier A, Collet G, Kieda C, Li T, Geib S J, Rosi N L and Petoud S 2013 Lanthanide near infrared imaging in living cells with Yb3+ nano metal organic frameworks *Proc. Natl. Acad. Sci.* **110** 17199–204

[173] Zheng T, Zhao J, Fang Z, Li M, Sun C, Li X, Wang X and Su Z 2017 A luminescent metal organic framework with high sensitivity for detecting and removing copper ions from simulated biological fluids *Dalt. Trans.* **46** 2456–61

[174] Rieter W J, Taylor K M L and Lin W 2007 Surface Modification and Functionalization of Nanoscale Metal- Organic Frameworks for Controlled Release and Luminescence Sensing *J. Am. Chem. Soc.* **129** 9852–9853

[175] Xia T, Zhu F, Jiang K, Cui Y, Yang Y and Guodong Q 2017 A luminescent ratiometric pH sensor based on a nanoscale and biocompatible Eu/Tb-mixed MOF *Dalt. Trans.* **46** 7549–55

[176] Zhao J, Wang Y, Dong W, Wu Y, Li D and Zhang Q 2016 A Robust Luminescent Tb(III)-MOF with Lewis Basic Pyridyl Sites for the Highly Sensitive Detection of Metal Ions and Small Molecules *Inorg. Chem.* **3** 3265−3271

[177] Abdelhamid H N, Bermejo-gómez A, Martín-matute B and Zou X 2017 A water-stable lanthanide metal-organic framework for fluorimetric detection of ferric ions and tryptophan *Microchim Acta* **184** 3363–71

[178] Dang S, Ma E, Sun Z-M and Zhang H 2012 A layer-structured Eu-MOF as a highly selective fluorescent probe for Fe3+ detection through a cation-exchange approach *J. Mater. Chem.* **22** 16920–6

[179] Yi X, Dong W, Zhang X, Xie J and Huang Y 2016 MIL-53 (Fe) MOFmediated catalytic chemiluminescence for sensitive detection of glucose *Anal. Bioanal. Chem.* **53** 8805–12

[180] Dong W, Liu X, Shi W and Huang Y 2015 Metal-organic framework MIL-53(Fe): facile microwave-assisted synthesis and use as a highly active peroxidase mimetic for glucose biosensing *RSC Adv.* **5** 17451–7

[181] Liu Y L, Zhao X J, Yang X X and Li Y F 2013 A nanosized metal-organic framework of Fe-MIL-88NH2 as a novel peroxidase mimic used for colorimetric detection of glucose *Analyst* **138** 4526–31

[182] Ai L, Li L, Zhang C, Fu J and Jiang J 2013 MIL-53 (Fe): A Metal-Organic Framework with Intrinsic Peroxidase-Like Catalytic Activity for Colorimetric Biosensing *Chem. Eur. J.* **19** 15105–8

[183] Zhang J-W, Zhang H-T, Du Z-Y, Wang X, Yu S-H and Jiang H-L 2014 Water-stable metal-organic frameworks with intrinsic peroxidase-like catalytic activity as a colorimetric biosensing platform *Chem. Commun.* **50** 1092–4

[184] Cui F, Deng Q and Sun L 2015 Prussian blue modified metal-organic framework MIL-101(Fe) with intrinsic peroxidase-like catalytic activity as a colorimetric biosensing platform *RSC Adv.* **5** 98215–21

[185] Yin Y, Gao C, Xiao Q, Lin G, Lin Z, Cai Z and Yang H 2016 Protein-Metal Organic Framework Hybrid Composites with Intrinsic Peroxidase-like Activity as a Colorimetric Biosensing Platform *Appl. Mater. Interfaces* **8** 29052−29061

[186] Yang S, Chen S, Liu S, Tang X, Qin L, Qiu G, Chen J-X and Chen W-H 2015 Platforms Formed from a Three-Dimensional Cu-Based Zwitterionic Metal − Organic Framework and Probe ss-DNA: Selective Fluorescent Biosensors for Human Immunode fi ciency Virus 1 ds-DNA and Sudan Virus RNA Sequences *Anal. Chem.* **87** 12206−12214

[187] Chen L, Zheng H, Zhu X, Lin Z, Guo L, Qiu B, Chen G and Chen Z 2013 Metal-organic frameworks-based biosensor for sequence-specific recognition of double-stranded DNA *Analyst* **138** 3490–3

[188] Liu C-S, Zhang Z-H, Chen M, Zhao H, Duan F-H, Chen D-M, Wang M-H, Zhang S and Du M 2017 Pore modulation of zirconium-organic frameworks for high-efficiency detection of trace proteins *Chem. Commun.* **53** 3941–4

[189] Wu X, Ma J, Li H, Chen D, Gu W, Yang G and Cheng P 2015 Metal-organic framework biosensor with high stability and selectivity in a bio-mimic environment *Chem. Commun.* **51** 9161–4

[190] Liu T, Hu R, Zhang X, Zhang K, Liu Y, Zhang X, Bai R, Li D and Yang Y 2016 Metal-Organic Framework Nanomaterials as Novel Signal Probes for Electron Transfer Mediated Ultrasensitive Electrochemical Immunoassay *Anal. Chem.* **88** 12516−12523

[191] Ling P, Lei J, Zhang L and Ju H 2015 Porphyrin-Encapsulated Metal−Organic Frameworks as Mimetic Catalysts for Electrochemical DNA Sensing via Allosteric Switch of Hairpin DNA *Anal. Chem.* **87** 3957−3963

[192] Tabar C T 2014 *Metal-Organic Frameworks for Drug Delivery Applications* (PhD Thesis submitted to the Univeersidad De Navarra)

[193] An J, Farha O K, Hupp J T, Pohl E, Yeh J I and Rosi N L 2012 Metal-adeninate vertices for the construction of an exceptionally porous metal-organic framework *Nat. Commun.* **3** 604–6

[194] Su H, Sun F, Jia J, He H, Wang A and Zhu G 2015 A highly porous medical metal – organic framework constructed from bioactive curcumin *Chem. Commun.* **51** 5774–7

[195] Burrows A D, Jurcic M, Keenan L L, Lane R A, Mahon M F, Warren M R, Nowell H, Paradowski M and Spencer J 2013 Incorporation by coordination and release of the iron chelator drug deferiprone from zinc-based metal-organic frameworks *Chem. Commun.* **49** 11260–2

[196] Levine D J, Runčevski T, Kapelewski M T, Keitz B K, Oktawiec J, Reed D A, Mason J A, Jiang H Z H, Colwell K A, Legendre C M, Fitzgerald S A and Long J R 2016 Olsalazine-Based Metal-Organic Frameworks as Biocompatible Platforms for H2 Adsorption and Drug Delivery *J. Am. Chem. Soc.* **138** 10143−10150

[197] Lu H, Yang X, Li S, Zhang Y, Sha J, Li C and Sun J 2015 Study on a new cyclodextrin based metal-organic framework with chiral helices *Inorg. Chem. Commun.* **61** 48–52

[198] Li H, Hill M R, Huang R, Doblin C, Lim S, Hill A J, Babarao R and Falcaro P 2016 Facile stabilization of cyclodextrin metal-organic frameworks under aqueous conditions via the incorporation of C60 in their matrices *Chem. Commun.* **52** 5973–6

[199] Cai H, Xu L, Lai H, Liu J, Ng S W and Li D 2017 A highly emissive and stable zinc(II) metal-organic framework as a host-guest chemopalette for approaching white-light-emission *Chem. Commun.* **53** 7917–20

[200] Katsoulidis A P, Park K S, Antypov D, Martí-gastaldo C, Miller G J, Warren J E, Robertson C M, Blanc F, Darling G R, Berry N G, Purton J A, Adams D J and Rosseinsky M J 2014 Guest-Adaptable and Water-Stable Peptide-Based Porous Materials by Imidazolate Side Chain Control *Angew. Chemie Int. Ed.* **53** 193–8

[201] Zhang J-H, Nong R, Xie S, Wang B, Ai P and Yuan L 2017 Homochiral metal-organic frameworks based on amino acid ligands for HPLC separation of enantiomers *Electrophoresis* **0** 1–8

[202] Radford R J, Lawrenz M, Nguyen P C, McCammon A J and Tezcan F A 2011 Porous protein frameworks with unsaturated metal centers in sterically encumbered coordination sites *Chem. Commun.* **47** 313–5

[203] Broomell C C, Birkedal H, Oliveira C L P, Pedersen J S, Gertenbach J-A, Young M and Douglas T 2010 Protein cage nanoparticles as secondary building units for the synthesis of 3-dimensional coordination polymers *Soft Matter* **6** 3167–71

[204] Sontz P A, Bailey J B, Ahn S and Tezcan F A 2015 A Metal Organic Framework with Spherical Protein Nodes: Rational Chemical Design of 3D Protein Crystals *J. Am. Chem. Soc.* **137** 11598−11601

[205] Sattar T and Athar M 2017 Hydrothermal Synthesis and Characterization of Copper Glycinate (Bio-MOF-29) and Its in Vitro Drugs Adsorption Studies *Open J. Inorg. Chem.* **7** 17–27

[206] Lu K, He C and Lin W 2014 Nanoscale Metal-Organic Framework for Highly E ff ective Photodynamic Therapy of Resistant Head and Neck Cancer *J. Am. Chem. Soc.* **136** 16712−16715